Mazumder Nirmal (Orcid ID: 0000-0001-8068-6484)

An insight into microscopy and analytical techniques for morphological, structural, chemical, and thermal characterization of cellulose

Ishita Chakraborty[1], Sintu Rongpipi[2], Indira G[1], Rakesh B[3], Sib Sankar Mal[4], Esther W. Gomez[2,5], Enrique D. Gomez[2,6,7], Ranjan Dutta Kalita[8], Yuthika Nath[9], Nirmal Mazumder[1,*]

[1]Department of Biophysics, Manipal School of Life Sciences, Manipal Academy of Higher Education, Manipal, Karnataka, India-576104

[2]Department of Chemical Engineering, The Pennsylvania State University, University Park, PA 16802

[3]Department of Life Science, CHRIST (Deemed to be University), Karnataka, India- 560029

[4]Department of Chemistry, National Institute of Technology, Karnataka, India- 575025

[5]Department of Biomedical Engineering, The Pennsylvania State University, University Park, PA 16802

[6]Department of Materials Science and Engineering, The Pennsylvania State University, University Park, PA 16802

[7]Materials Research Institute, The Pennsylvania State University, University Park, PA 16802

[8]Department of Biotechnology, Royal Global University, Guwahati, Assam, India-781035

[9]Department of Serology, State Forensic Science Laboratory, Kahilipara, Guwahati, Assam, India, Pin: 781021

***Corresponding author:** nirmaluva@gmail.com

ORCID ID- 0000-0001-8068-6484

ABSTRACT

Cellulose obtained from plants is a bio-polysaccharide and the most abundant organic polymer on earth that has immense household and industrial applications. Hence, the characterization of cellulose properties is important for determining its appropriate

applications. Here, we review the characterization of cellulose morphology, surface topography using microscopic techniques including optical microscopy (OM), transmission electron microscopy (TEM), scanning electron microscopy (SEM), and atomic force microscopy (AFM). Other physicochemical characteristics like crystallinity, chemical composition, and thermal properties are studied using techniques including X-ray diffraction (XRD), Fourier transform infrared (FTIR), Raman spectroscopy, nuclear magnetic resonance (NMR), differential scanning calorimetry (DSC), and thermogravimetric analysis (TGA). This review may contribute to the development of using cellulose as a low-cost raw material with anticipated physicochemical properties.

Keywords: Cellulose. Crystallinity. Electron microscope. Differential scanning calorimetry. Fourier transform infrared spectroscopy. Thermogravimetric analysis

Research Highlights:

- Morphology and surface topography of Cellulose structure is characterized using microscopy techniques including optical microscopy (OM), transmission electron microscopy (TEM), scanning electron microscopy (SEM), and atomic force microscopy (AFM)
- Other analytical techniques used for physicochemical characterization of cellulose include XRD, FTIR, Raman, NMR spectroscopy, DSC, and TGA

1. INTRODUCTION

Cellulose is an insoluble dietary fiber obtained from plants consisting of poly(1,4-β-D-anhydroglucopyranose) units (Choi, Kang, Lim, & Chang, 2018). It is the most abundant biopolymer in nature and has wide applications in various fields such as construction, textiles, paper, medicine, and packaging. Natural cellulose fibers are obtained from plant sources, mainly cotton, flax, hemp, jute, and ramie. The ultrastructure of cellulose fibers shows the hierarchical arrangement, starting from elementary fibers to micro and macrofibres, as shown in **Fig. 1** (Chinga-Carrasco & Syverud, 2010; Fratzl & Weinkamer, 2007; Kaushik, Fraschini, Chauve, Putaux, & Moores, 2015). Cellulose exists in four completely different polymorphs, cellulose I, II, III, and IV with varied characteristics, as summarised in **Table 1.** To use cellulose for various purposes, it needs to be extracted and isolated from its source, followed by purification and modification. These methods of extraction, purification, and modification affect chemical reactivity and physical properties of cellulose, such as thermal stability, mechanical performance, solubility, the quantity of inter and intra-molecular hydrogen bonds, the chain lengths and their distribution, the crystallinity, and the distribution of functional groups in the repeating monomers of the polymer. These physical and chemical properties play a major role in determining the use of cellulose from an industrial and commercial point of view (Kalita, Nath, Ochubiojo, & Buragohain, 2013). Therefore, it is important to be up to date on techniques used for cellulose characterization and to collect reliable data on cellulose characteristics for quality control and research development purpose. Several microscopy, spectroscopy, and analytical techniques have been employed so far to study the architectures, morphology, and properties of fibrillar units from native and modified cellulose (Table 2). **Table 2**. depicts a compilation of various techniques used to study cellulose along with the characteristics studied. Choi et al., 2018 reported the characterization of cellulose, extracted from the wastes of Graviola (*Annona muricata*.) leaf

using Fourier transform infrared (FTIR) spectroscopy, nuclear magnetic resonance (NMR), X-ray diffraction (XRD), and scanning electron microscopy (SEM) (Choi et al., 2018). The morphology and topography of both native and modified cellulose have been studied using microscopy techniques, such as SEM, and atomic force microscopy (AFM). SEM and TEM elucidate the surface microstructure such as voids and cracks present on the surface. It reveals the changes in morphology post hydrolysis via various agents, which also alters the physicochemical and thermal properties of cellulose. AFM usually elucidates the three-dimensional surface topography based on parameters like surface roughness. XRD is another technique that has been used widely to study cellulose crystallinity in native and modified cellulose (Hanley, Revol, Godbout, & Gray, 1997; Ye et al., 2020; Zhao et al., 2007). The vibrational spectroscopy (FTIR) and NMR spectra are used to study its molecular structure and reveal the presence of impurities like lignin and pectin. The thermal stability of cellulose depends on various factors, such as crystallinity, inter and intramolecular hydrogen bonding, and hydration. The thermal stability can be estimated from peak gelatinization temperature and gelatinization enthalpy, which are obtained using differential scanning calorimetry (DSC) (Awal, Ghosh, & Sain, 2010). Natural cellulose consists of both crystalline and amorphous domains in different proportions based on its source and origin. During any chemical modification, acids, chemicals, or enzymes affect the less ordered and peripheral amorphous domain and are unable to access the crystalline regions (Ciolacu, Ciolacu, & Popa, 2011). It is therefore important to study their mode of action and their effect on cellulose fibers. This review is a broad overview of the microscopic, spectroscopic, and analytical techniques including OM, SEM, TEM, FTIR, Raman spectroscopy, XRD, NMR, DSC, and TGA used for characterization of cellulose concerning its structure and morphology, crystalline nature, chemical, and thermal properties, and the changes that occur during various modifications.

2. MICROSCOPY TECHNIQUES

Different structures and morphologies of cellulose fibers can impact the properties of the end material. Therefore, a better understanding of the morphology of natural or modified fibers is necessary for developing cellulose fiber-reinforced products. Several microscopy techniques have been used to elucidate the morphology of cellulose fibers.

2.1 OPTICAL MICROSCOPY

Microscopy techniques have been employed to analyze the morphological and structural properties, including the size and shape of a single cellulose fiber or the fiber network. Optical microscopy (OM) is an imaging technique that uses visible light to illuminate the sample. OM has been used to study dispersion, swelling, and staining of cellulose fiber, using both unpolarized and polarized light (Chakraborty, Pallen, Shetty, Roy, & Mazumder, 2020; Rollins & Tripp, 1954). OM has revealed the vast differences in sizes of isolated, microcrystalline cellulose (MCC) and nanocellulose particles (Vanderghem, Jacquet, Danthine, Blecker, & Paquot, 2012). Further, it has helped to closely observe the mechanism of enzymatic degradation and dissolution of cellulose fibers. For example, lytic polysaccharide monooxygenases (LPMOs) are strong oxidative enzymes that break down polysaccharides such as cellulose. Since cellulose fibrils have a highly interlaced network, they need to be dispersed or separated from each other. Native fibers are 10 micrometers in diameter and around 1 mm in length. However, LPMO treatment and dispersion resulted in fiber delamination into thinner and shorter structures compared to the native fibers (Villares et al., 2017). The dissolution mechanisms observed under OM are mostly similar for all cellulose fibers irrespective of their botanical origin including wood, cotton, other plant fibers. OM revealed that the dissolution of cellulose in the NaOH/water system occurs in two steps- dismantlement and fragmentation and these steps are governed by the swelling and the shearing of the original fiber structure (Le Moigne & Navard, 2010). OM study of

deconstruction and degradation of cellulose contributes to understanding the global carbon cycling and environmental concerns. Since cellulose is essential for paper and textile industries; the tensile strength of the cellulose fibers is an important factor for cellulose-derived products. The tensile strength further depends on the strength of the pulp fiber and the fiber-to-fiber bonds that are determined by polarized light microscopy (PM) due to the birefringence possessed by the fibers (Gilli, Kappel, Hirn, & Schennach, 2009).

Birefringence is the behaviour of molecularly ordered or crystalline materials, which demonstrate two refractive indices for the two polarizations of incident light and is a significant optical factor for characterizing cellulose. Orientation birefringence of different cellulose is studied using optical birefringence analyzers. Cellulose fibers appear bright on the transmission of polarized light if the transmitted light and fibers lie at an angle of 45°. However, if the direction of fibers and the transmission of light is either parallel or normal to each other, the fibers exhibit minimal intensity, and the bonded areas appear brighter than the single fiber (Gilli et al., 2009). Cotton and vegetable fibers show strong double refraction under polarized light. Thus, the study of birefringence using polarization microscopy is also indicative of fiber orientation. Cellulose fibers derived from cotton are twisted and wrinkled due to the uneven collapse of its cellulosic tube. However, the standard birefringence of the cotton fiber is because of its extraordinarily orientated macromolecular shape. Refractive index measurements showed that the positive birefringence is because maximum chains in the fiber lie parallel and perpendicular to the axis (Titus, Staud, & Gray, 1932). Deguchi et al., 2006 reported the birefringent properties of fibrous cellulose during heating in the presence of water using PM. A negative correlation between the birefringence of the cellulose fibers and the increasing temperature was exhibited (**Fig. 2**) (Deguchi, Tsujii, & Horikoshi, 2006). Birefringence was retained up to 310ºC, which was visualized using pseudo color under cross polarizers. It was observed that the transformation of crystalline cellulose to

amorphous occurs at 320 ºC. Polarized micrographs revealed no changes in cellulose fiber shape until 325 ºC. Beyond these temperatures, specifically at 340 ºC, dissolution of cellulose fibers occurred, and complete loss of birefringence was observed**.** This total loss of birefringence with increasing temperature was due to fiber deformation and loss of organization in the fiber as shown in **Fig. 2**. As a result of the transformation and large deformation, the cellulose fibers were finally converted into a plastic-like solid. This resulted in a drastic change in the cellulose's mechanical and chemical properties.

However, a drawback with conventional OM is the limited ability to create three-dimensional image reconstruction, because the manual placing of each slice of the sample would be required (Hawinkels, Beex, & Peerlings, 2009). OM provides preliminary information on the ultrastructure and molecular structure of cellulose and its variation with various treatments, which is required for textile fiber identification (Garside & Wyeth, 2006).

2.2 NON-LINEAR OPTICAL MICROSCOPY

Non-linear optical microscopy (NLOM) is particularly applied to study of cellulose at sub-cellular resolution compared to linear optical microscopy. NLOM uses nonlinear interactions between light and material to provide images with intricate details and superior contrast. Second harmonic generation (SHG) and coherent anti-Stokes Raman scattering microscopy are used for the detailed structural characterization of polysaccharides such as starch and cellulose from various sources (Govindaraju et al., 2021; Govindaraju et al., 2022; Mazumder et al., 2013). Since electron microscopy and scanning probe microscopy are not efficient enough to analyze the details of molecular structure and specificity, non-linear microscopy techniques come into play. In addition, non-linear microscopy techniques does not have complicated sample preparation in comparison to electron microscopy. A combination of CARS and SHG microscopies offers thorough information about the internal structure and

composition (Mazumder et al., 2019). In SHG microscopy mode, two photons of same frequency interact with the nonlinear sample and produces another photon that has double the frequency and half the wavelength of the initial photons. Samples like cellulose and collagen with non-centrosymmetric structures give out SHG signals and can be exposed to SHG microscopy (Mazumder et al., 2019). In another study the macromolecular structure of bacterial cellulose from Valonia and Acetobacter were studied using second-harmonic generation (SHG) imaging microscopy. The cellulose microfibrils in each lamella were very well aligned and ordered. The second-order nonlinear response is very sensitive to orientation and anisotropy of cellulose fibers. As reported by Slepkov et al., a robust CARS signal was observed in cellulose fibres along with C-H stretch (2750 cm^{-1}–2970 cm^{-1}), due to the intramolecular structure. the O-H stretch region gave signals (3000 cm^{-1}–3400 cm^{-1}) that was accredited to intermolecular hydrogen bonding structure (Slepkov, et al., 2010). In CARS microscopy, intensity signals depend on the density of CH_2 groups in a nonlinear fashion. This indicates that higher CARS signal is obtained from higher density of CH_2 group, which in turn is proportional to the amount of β-(1,4)-D-glucan polymers in present in cellulose (Slepkov, et al., 2010).

Nonlinear optical imaging techniques are extremely suitable for material characterization due to their non-destructive in nature, label free and high penetration depth capability. Since cellulose is hydrophilic, its crystalline properties are impacted by water and molecular alignment. Hydration maintains the features in the CH-stretching region of cellulose. Raman spectroscopy and CARS microscopy were combined with SHG to examine the C-H stretching modes in dry and hydrated cellulose fibres from various sources (Zimmerley et al., 2010). In cotton fibres, the orientation of methylene groups remains unaffected, indicating a high degree of order. On the other hand, the methylene groups in rayon fibres were directed perpendicular to the fibre axis. Further, hydration, did not affect the orientation of fibres

suggesting that water does not affect the alignment of the polyglucan chains of the cellulose fibres (Zimmerley et al., 2010). **Fig. 3 a and b** depicts nonlinear optical microscopy images of cellulose fibres obtained from three different cellulose-rich substrates-Pulp fibre, acid-treated fibre (AT fibre), and Avicel (Peciulyte et al., 2016). Nonlinear optical microscopy provides structural as well as chemical contrast without any external labelling.

However, optical microscopy has its limitations when it comes to obtaining higher resolution images and three-dimensional images. Therefore, scanning electron microscopy is opted to examine the ultrastructure of cellulose in detail.

2.3 ELECTRON MICROSCOPY

Electron microscopy overcomes the resolution limits of OM and enables a high-resolution, three-dimensional study of the ultrastructure of cellulose since it provides a greater depth of field. It uses a beam of electrons to magnify the image of a sample**.** However, sample preparation for electron microscopy requires a destructive process and can be arduous and time-consuming. SEM or TEM is used depending on the type of information needed. SEM helps to study and compare the surface structures, morphology, and fibril diameter of native and modified cellulose. The variability observed in the size of reported cellulose fibers is due to the bundling of elementary fibers into microfibrils which further agglomerate into macro fibrils. The variation in the number of these elementary fibers may result in different sizes of fibrils reported in the literature. SEM is used for the 3D reconstruction of cellulose fibers (Chinga-Carrasco & Syverud, 2010; Ding, Zhao, & Zeng, 2014; N.J. Heyn, 1969). SEM studies of individual cellulose fibers show wrinkles, grooves, and fissures, which are the characteristic features of its surface topography. It also clearly shows the shape and size distribution of the microfibrils in cotton linters. Cellulose fibers from native arecanut husk and cassava pulp show an uneven structure of fiber and the presence of various binding

particles like hemicellulose, and lignin, as observed in **Fig. 4a, d** (Chandra, George, & Narayanankutty, 2016). **Fig. 4 b, e** exhibit that alkali treatment of cellulose modifies the surface morphology eradicating the lignin, hemicellulose, and external surface fibers. **Fig. 4c** shows the complete defibrillation of cellulose fibers due to acid treatment. Bleaching makes the fiber smooth and gives a uniform fibril surface due to the removal of all the non-cellulosic material. The bleaching treatment also separates the fiber bundles into individual fibers and removes all the non-cellulosic and binding substances, facilitating the separation of fibers (**Fig. 4f)**. A field emission scanning electron microscope (FESEM) can be used to observe the disintegration of cellulose microfibrils due to bleaching, acid, or alkali treatment. Acid treatment of cellulose fibers reduces its size to a nanometer scale with a diameter ranging from 15-20 nm and an aspect ratio in the range of 10-15 (Johar, Ahmad, & Dufresne, 2012). The aspect ratio of a nanomaterial influences its viscosity in suspension and plays an essential part in determining the performances of cellulose nanocrystal (CNC) based polymers, functional materials, and suspensions (Rashid, & Dutta, 2020). Several software programs have been used to analyze features of cellulose from SEM micrographs. Programs like EZE Image, MeXTM, and 3D TOPx have been developed to investigate surface topography using SEM 3D stereo microscopy (Marinello, Bariani, Savio, Horsewell, & De Chiffre, 2008; Ponz, Ladaga, & Bonetto, 2006). Apart from SEM, TEM was also used to obtain dimensions of cellulose nanofibers produced by dual-acid hydrolysis **(Fig. 5 a, b).** Cellulosic nanofibers obtained through hydrochloric acid (HCl) treatment have a diameter of about 1 μm. In contrast, the nanofibers from sulphuric acid (H_2SO_4) treatment showed a length and diameter in the range of 8-15 nm and 200-800 nm, respectively. This indicates electron microscopy can differentiate between the hydrolysis efficiency of different acids (Ruangudomsakul, Ruksakulpiwat, & Ruksakulpiwat, 2015). Several studies have used a combination of both SEM and TEM to characterize native and modified cellulose nanofibers. Cellulose nanofibrils

from wheat straw were isolated by steam explosion. The SEM studies showed individual nanofibers after chemical treatment due to the removal of cementing particles like lignin, pectin, and hemicellulose surrounding the fiber bundles. TEM images also showed defibrillation of cellulose nanofibrils from the fiber bundles. The average diameter of these nanofibrils was found to be between 10-15 nm, which is lower than the fiber bundles. The nanofibrils size from wheat straw was found to be in the range of 10-60 nm (Kaushik & Singh, 2011). The cellulose nanofibrils from the raw pineapple leaf fibers were extracted by steam explosion method followed by bleaching to remove the cementing particles like lignin and hemicellulose. SEM study was used to visualize the defibrillation and formation of nanofibrils. TEM studies revealed cellulose nanofibrils possessed width in the range of 5-60 nm range (Cherian et al., 2010). Similar observations were made in the case of cellulose nanocrystals obtained from tea leaf wastes. SEM studies revealed alkali causes defibrillation followed by acid hydrolysis that finally splits the fibers into nanoparticles TEM studies revealed these rod-like cellulose nanocrystals had an average diameter of 7.9 nm. Also, it was noted that these nanocrystals tend to aggregate due to the surface ionic charge that they possess (Rahman, Chieng, Ibrahim, & Rahman, 2017). Electron microscopy also revealed the mechanism of enzymatic treatments, cellulase treatment reduced the average fiber length due to weaker junctions along the length of cellulose fibers that can be easily degraded by the activity of enzymes. TEM analysis showed that enzymatic treatments did not affect the cellulose nanocrystal length but reduced the nanocrystal's width with the aspect ratio remaining between 12-15 without any significant changes (Beyene et al., 2018; Jenkins & Donald, 1997). Two endemic rice husk varieties (*Ahu and Boro*) were subjected to the hydrothermal process, followed by bleaching and acid treatments. TEM studies revealed the average diameter of the CNC post-acid treatments to be around 30-40 nm as depicted in **Fig 5 c, d** (Kalita et al., 2015). Electron microscopy is indispensable when it comes to studying

fiber-based products and their interaction with various compounds. For instance, SEM images of paper surfaces developed from cellulose fibers helped to identify the other sizing agents and fillers that have been utilized in production (Wu et al., 2014). The same can be used in textile industries to identify various sources of raw materials used. Studying the changes in cellulose fiber structure, and the mechanism of hydrolysis aids in a better understanding of its chemical composition, physiological functions, and applications. Nevertheless, optical and electron microscopes are unable to provide clear topographical characterization. Therefore to obtain the molecular scale features on the surface of the sample, AFM is preferred over optical and electron microscopy.

2.4 ATOMIC FORCE MICROSCOPY

Atomic force microscopy (AFM) is a non-destructive, near-field type imaging technique that can create 3D images of surface topography and various interaction forces with atomic and sub-atomic resolution. It generates an image of a surface by measuring force interactions between the sample and a small sharp tip on the end of a flexible cantilever that scans across the sample surface**. Fig 6a** shows the contact between an AFM probe and the surface of the cotton fiber. The AFM tip's vertical movement can be monitored by a laser beam reflected off the back of the tip onto a photodetector grid (Henderson, 1994; Pesacreta, Carlson, & Triplett, 1997). AFM in combination with other techniques including SEM and molecular dynamic stimulations reveals the complex hierarchical structure of cellulose that consists of individual macromolecules forming elementary fibrils and aggregate into microfibrils. These building blocks are across dimensions ranging from a few nanometers to tens of microns (Paiva, Sequeira, Evtuguin, Kholkin, & Portugal, 2007). Apart from the ability of AFM to create 3D images of the topology of these structures, it has several advantages over SEM and TEM, such as scanning under different controlled environments, including hydrated and atmospheric conditions, with minimal sample preparation. Besides structural details, AFM

can provide information on surface forces such as adhesion, friction, electrostatic forces, and van der Waals forces, and reveal mechanical and chemical maps such as deformation maps, and chemical composition maps (Hosseinali & Thomasson, 2019; Prats-Mateu & Gierlinger, 2017). **Fig. 6** depicts the topography (b), deformation(d), and adhesion maps (c) of cotton fibers obtained in the force tapping mode. AFM has been used since the early 1990s in cellulosic research when Valonia microfibrils were first imaged (Hanley et al., 1997). It was able to identify monoclinic structures at the molecular level (Kuutti, Peltonen, Pere, & Teleman, 1995). Later, the triclinic allomorph cellulose Iα was visualized by AFM imaging of Valonia fibril (Baker et al.,1997). Since then, AFM has been used to examine more complex cellulose samples such as wood or cotton fibers, paper, and related materials. It has been very often used to characterize the surface morphology of cellulose fibers at high resolution under ambient conditions. The measurements show periodicities along the microfibril axis that correspond to the fiber and glucose unit repeat distances (Hanley, Giasson et al. 1992, Baker, Helbert et al. 1998) . Two-dimensional Fourier analysis of AFM raw data could provide cellulose crystal parameters. Compared with an artificial cellulose surface generated from modeling, it has been used to identify crystal faces of cellulose Iβ from *Valonia macrophysa* with a resolution of 0.4 nm (Kuutti et al., 1995). A real-time AFM study of structural changes in Valonia cellulose crystals acted upon by an exocellulase enzyme, cellobiohydrolase I (CBH I) found that cellulose surface roughness increased, and the overall size of the crystal decreased after adding the enzyme. Interestingly the size reduction occurred only in the width of the crystal and not in height. At the same time, the cellulose cross-section also changed from asymmetric to nearly symmetric. This provided evidence to support the hypothesis that exocellulase hydrolyzes only the hydrophobic faces of cellulose. AFM has also been able to distinguish between the effects of exoglucanase (CBH I) and endoglucanase (EG II) on the surface of cotton fibers (Lee, Evans, & Woodward,

2000). It revealed that treatment with CBH I resulted in the appearance of distinct pathways or tracks along the length of the microfibril while treatment with EG II caused peeling and smoothing of the fiber surface. The surface roughness of cellulose fibers is quantified through several parameters such as the root mean squared (RMS) or standard deviation of the height (Z) data; the surface area deviation (SAD), or the increase in the total surface area within the scanned area compared to a flat surface having the same horizontal dimensions; the total power (TP) or total amplitude derived from an integration of the fast Fourier transform of the image; and the fractal dimension (FRAC) of the entire surface of each scan. These have been used to examine effects on cotton fibers' surface morphology following treatments by chemicals such as peroxide, alkali, acid, and alkali/acid (Pesacreta et al., 1997). The surface roughness value ranged from 3556 to 13080 nm for TP, 42.03 to 78.94 for RMS, 8.35 to 16.13 nm for SAD, and 2.118 to 2.162 nm for FRAC for 6.25 μm^2 area scans. The study suggested that chemical treatments do have a significant effect on surface roughness and cotton fibers treated with alkali/acid have smaller roughness values. AFM allows the study of inter-particle forces in controllable environments. It has been used to examine cellulose surface interactions to gain insights into interfacial phenomena in cellulose applications (Nigmatullin et al., 2004; Rutland, Carambassis, Willing, & Neuman, 1997; Zauscher & Klingenberg, 2000). For example, AFM in peak force tapping mode has been used to characterize adhesion in two different cotton fibers. The adherence of the two cotton varieties could be compared through Gaussian fits of the adhesion distributions, and they were found to be significantly different, as shown in **Fig. 6c**. AFM has also been used to examine the interaction of cellulose-binding domains with cellulose, which is expected to alter cellulose surface chemistry (Nigmatullin et al., 2004). It has also been used to determine binding sites and the strength of interactions between compatibilizers and cellulose rich wood fibers while synthesizing incompatible composites such as wood plastic composites (Effah, Van Reenen

et al. 2015). Compatibilizers are used to alter the wood fibres surface to improve their affinity towards other fillers. Furthermore, AFM has been used to characterize cellulose fibers' mechanical properties, such as flexibility, and elasticity (Pettersson, Hellwig et al. 2017, Hellwig, Durán et al. 2018). A few examples of such studies involve measuring flexibility and modulus of elasticity for never dried cellulose fibers in bleached softwood kraft pulp and thermomechanical pulp using a direct force-displacement method and measuring Young's modulus of pulp fibers in liquid through indentation and a linearized Hertz model (Hellwig et al., 2018; Pettersson et al., 2017). Flexibility (F) and modulus of elasticity (E) for never dried cellulose fibers in bleached softwood kraft pulp and thermomechanical pulp were measured by using beam model of cellulose fibers (Pettersson et al., 2017). Flexibility is expressed as $F = \frac{1}{EI} = \frac{3\delta_B}{PL^3}$ where I is the moment of inertia (a function of the cross-sectional geometry of the fibers), δ_B is deflection of beam, P is point load, and L is beam length. So, we can calculate flexibility from force-displacement method if length of fiber is known and also, the modulus of elasticity if cross-sectional geometry of fiber is known. Young's modulus of never-dried fully bleached kraft pulps has also been measured by fitting force vs. indentation profiles, obtained from AFM to a contact mechanics model called Hertz model (Hellwig et al., 2018). The study used a linearized Hertz model for simplification as it obviates the need to know the exact point of contact between the sample surface and probe of the AFM.

Another such study examined the deformation of two different cotton fibers in peak force tapping mode and compared them through Gaussian fits of the deformation distributions (Hosseinali & Thomasson, 2019). The difference in deformation between the two fibers was statistically significant, as shown in **Fig. 6d.** AFM has the unique capability of carrying out the simultaneous morphological and chemical characterization of a surface. Using tapping (intermittent contact) mode imaging, it can distinguish variation in surface composition through detecting variation in local visco-elastic properties within a sample. This technique

could differentiate between lignin-rich and cellulose-rich regions in the wood pulp after the delignification process (Kino & Corle, 1996). More specific surface interactions properties can be studied through interactions between surface and chemically modified tips and texture. This scanning surface method with modified AFM probes is called chemical probe microscopy (CFM) (Bastidas et al., 2005; Noy, Vezenov, & Lieber, 1997). AFM tips modified with -COOH, -CH_3, and -OH functional groups have been successfully applied to study adhesion forces on cellulose model surfaces and bleached softwood kraft pulp fibers in aqueous media (Bastidas et al., 2005). The study investigated the effects of pH on adhesion forces measured by these modified tips. It found that the adhesion forces are dependent on pH for -COOH terminated tips, but for the –CH_3 and –OH terminated tips, adhesion is not strongly affected by pH. Adhesion between fibers and polymers in composite materials strongly affects the mechanical properties of the final composite. The adhesion of fibers can be enhanced through several chemical treatments such as sodium hydroxide, sodium hydroxide plus acetic anhydride, and formic acid (Baley, Perrot, Busnel, Guezenoc, & Davies, 2006; Baley, 2002). AFM has been used to directly measure surface roughness and adhesion forces in flax fibers (Balnois, Busnel, Baley, & Grohens, 2007). The chemical treatments made no significant changes to the surface roughness of fibers. Still, they influenced the adhesion forces differently, such as sodium hydroxide-based treatment, which increased the adhesion force between the fiber and the AFM tip. In contrast, the formic acid-based treatment decreased the adhesion force. Colloid probe (CP) AFM has been widely adopted to study interaction forces in cellulose-based materials. This technique involves modifying the tip of an AFM probe to a semi-spherical shape or attaching a single spherical colloid to a tipless AFM cantilever probe (Lai, Zhang, Sugano, Xie, & Kallio, 2019). Commonly, CP AFM measures interaction forces under AFM modes, such as pull-off mode (POM) and force volume mode (FVM), including collecting plots of force as a function of

probe displacement along the axis perpendicular to the surface. CP AFM has been used to study the interaction between xyloglucan and cellulose, which is of considerable interest as xyloglucan can act as a molecular anchor to tether chemical functionality to cellulose for industrial plant fiber modifications (Zhou, Rutland, Teeri, & Brumer, 2007). These studies were carried out by attaching cellulose particles to an AFM cantilever. For example, an analysis of AFM of adsorption of tamarind xyloglucan on cellulose surfaces revealed that roughness and crystallinity affect friction and adhesion in an aqueous environment. It also found that xyloglucan adsorption on cellulose reduced friction and enhanced adhesion (Stiernstedt, et al., 2006; Stiernstedt, Brumer, Zhou, Teeri, & Rutland, 2006). Another study exhibited the impact of arabinoxylan and xyloglucan on interactions between nanoscale cellulose fibers in a hydrated bacterial cellulose network. It was observed that xyloglucan or arabinoxylans presence accelerated the adhesive energy by 4.3 and 1.3-fold, respectively, that is expected with two hemicellulose polysaccharides having one-of-a-kind specificity of hydrogen bonding with cellulose.

Obtaining an adhesion map from POM and FVM modes can be very time-consuming, so more recently, CP AFM in peak-force mode (PFM) has been applied to study cellulose-cellulose interaction. It provides the benefit of acquiring force curves with high precision force control (Lai et al., 2019). A unique capability of AFM is that it can image living tissues in near-physiological conditions with minimal alteration of the sample. It has been used to image isolated cell walls of several plants such as apple, water chestnut, potato, carrot, cotton, and celery parenchyma (Kirby, Gunning, Waldron, Morris, & Ng, 1996; Pesacreta et al., 1997;). It has also been used to examine the organization of cellulose microfibrils in primary cell walls of onion (*Allium cepa* L.) and *Arabidopsis thaliana* (Kafle et al., 2014; Xiao, Zhang, Zheng, Cosgrove, & Anderson, 2016; Zhang, Mahgsoudy-Louyeh, Tittmann, & Cosgrove, 2014; Zhang, Vavylonis, Durachko, & Cosgrove, 2017). AFM images showed that

cellulose microfibrils orientation and alignment appear more dispersed in younger scales compared with older scales (Kafle et al., 2014; Zhang et al., 2014). AFM-based nanomechanical maps also revealed significant heterogeneity in cell wall stiffness and adhesiveness at the nanometer scale (Xiao et al., 2016). Insights into microfibril movements and connectivity could also be obtained through AFM of mechanically stretched and enzyme-treated cell walls (Zhang et al., 2017). Simultaneous morphological and chemical information has been extracted from cellulosic samples using AFM in combination with other techniques such as X-ray photon spectroscopy (XPS), time-of-flight secondary mass-ion spectroscopy (ToF-SIMS), and total internal reflectance fluorescence microscopy (TIRFM) (Eronen, Österberg, & Jääskeläinen, 2009; Fardim, Gustafsson, Schoultz, Peltonen, & Holmbom, 2005; Gustafsson, Ciovica, & Peltonen, 2003). Hybrid techniques such as AFM-IR allow simultaneous acquisition of chemistry, structure, and mechanics of cellulose-lignin films in the submicron to the nano-scale range, and AFM-Raman could also examine chemical and morphological changes in the mercerization of cellulose in filter papers (Eronen et al., 2009; Prats-Mateu & Gierlinger, 2017). It revealed swollen and more granular microfibrils in cellulose II (mercerized cellulose) compared to cellulose I and could also detect changes in microfibril orientation on the sample surfaces. Nowadays, superior AFM programs like high-resolution AFM (HS-AFM) permit direct visualization of the shape and dynamics of organic molecules at temporal resolution. It has been used to study the mechanism through which cellulase attacks cellulose fiber (Chary & Srivastava, 2013). AFM has hence proven to be very useful in characterizing surface morphology and interactions of cellulose fibers. AFM images, however, are created from a scanning probe mechanism that is prone to artifacts arising from cross-talks between topographic and other signals caused by the gap-width control mechanism (Yarbrough, Himmel, & Ding, 2009). AFM data of cellulose fibers are most affected by tip artifacts. The tip's triangular shape, mostly the sharpness of the tip's apex

and sidewall angle, can significantly affect the lateral dimensions of objects being imaged. Detailed discussion on determining artifacts and overcoming them has been reported in the literature, and the applications of those are recommended for better accuracy of AFM data (Hoffmann, Jungk, & Soergel, 2007; Ricci & Braga, 2004; Sedin & Rowlen, 2001).

Since cellulose is widely used by the industries to produce food, lumber, paper, textile and packaging, it is important to comprehend its structural and functional elements, beyond its morphology. It is essential to study in detail the effects by thermal, chemical and biochemical processes on the properties of cellulose which is beyond the capacities of microscopy techniques. Hence, non-imaging techniques such as X- ray diffraction, Fourier transform infrared spectroscopy, Raman spectroscopy, nuclear magnetic resonance, and thermoanalytical techniques come into play for detailed characterization of cellulose.

3. NON IMAGING ANALYTICAL TECHNIQUES

3.1 X-RAY METHODS

XRD is an analytical technique used for characterizing crystalline or semi crystalline materials. It is established on constructive interference of monochromatic X-rays and the sample**.** It provides information on the crystal structure, phases, preferred crystal orientations (texture), and other structural parameters, such as average size, crystallinity, strain, and crystal defects (Chakraborty, Govindaraju, Rongpipi, Mahato, & Mazumder,2021; Ward, 1950). It is invaluable for characterizing the crystalline structure of cellulose fibers. Several cellulose crystal structure parameters and organization parameters can significantly impact the chemical and physical properties of cellulose fibers. XRD has been widely used to characterize the parameters, such as (1) nature of crystal lattice, i.e., cellulose polymorphism, (2) percentage of crystalline material, i.e., degree of crystallinity, (3) size of crystallites, and (4) orientation of crystallite (Bunaciu, Udriştioiu, & Aboul-Enein, 2015; Ward, 1950).

Crystal parameters such as the unit cell dimensions, crystal coherence length, amount of crystalline material, and orientation of crystallites can be determined from the intensity and shape of diffraction profiles (Kim, Lee, & Kafle, 2013; Rongpipi, Ye, Gomez, & Gomez, 2019).

Chemical treatments such as sodium hydroxide treatment (mercerization) and liquid ammonia treatments cause cellulose crystal polymorphic changes in fibers (Atalla & Nagel, 1974; Mittal, Katahira, Himmel, & Johnson, 2011). However, this influences several physical properties like dyeability and mechanical strength (Ishikawa, Okano, & Sugiyama, 1997). XRD can characterize cellulose polymorphs through their unique XRD spectra, as shown in **Fig. 7a.** Cellulose I from Avicel shows two distinct peaks with where the second peak shows higher intensity. The sharpness of the second peak is seen to be reducing in subsequent cellulose II. Further, a small shoulder peak appears to the right in case of cellulose III. It has been used to correlate polymorphic cellulose structures with fiber properties after chemical treatments. Studies have found that the mercerization process used in the cotton textile industry has minimal effects on polymorphic changes and physical property improvements. Simultaneously, the presence of liquid ammonia confirmed improved smoothness, wrinkle recovery, flex abrasion, and tear strength, even though the tensile power decreased. These modifications have been attributed to a few conversions to cellulose III and a reduction in crystallinity (Kafle et al., 2014). Crystallinity affects mechanical properties such as the strength and stiffness of cellulose and cellulose-derived material (Rongpipi et al., 2019).

Several fiber properties such as extensibility, moisture regain, density, and chemical reactivity are also impacted by the change in the degree of crystallinity, which is defined as the percentage of crystalline material in a sample, i.e., the ratio of crystalline to crystalline plus amorphous content by volume (Ward, 1950). Crystallinity is described through a

parameter called the crystallinity index (CI), and XRD is the most widely used technique to measure the CI of cellulose. The general formula for determining the CI from XRD is:

$$CI = I_c/(\frac{I_c}{I_a}) * 100 \quad (1)$$

Several methods for estimating the CI of cellulose from XRD spectra have been described in detail in the literature (Ahvenainen, Kontro, & Svedström, 2016; Kim et al., 2013; Park, Baker, Himmel, Parilla, & Johnson, 2010; Rongpipi et al., 2019; Thygesen, Oddershede, Lilholt, Thomsen, & Ståhl, 2005). These methods involve either calculating relative peak intensities of crystalline to amorphous cellulose (Segal method shown in **Fig. 7b** or relative peak areas of crystalline cellulose to total peak area (peak deconvolution method and Ruland-Vonk method). There are also other approaches to determine the CI of cellulose, such as Hermans–Weidinger method and the Debye method (Gusev, 1978; Ling et al., 2019). However, they have been less widely used as compared to the above-mentioned. The Segal peak height method is the simplest and the most prevalent method for estimating cellulose crystallinity (French, 2014; Ling et al., 2019). **Fig. 7b** shows XRD spectra of Avicel PH-101 illustrating the Segal method of determining cellulose crystallinity. The cellulose peaks are indexed according to the convention in which the unit cell has the c-axis vertical, the *a*-axis towards the viewer, and the *b*-axis towards the right, and *a* being shorter than *b* (French, 2014). The Segal method defines CI as the ratio of difference of maximum intensity (intensity of (200) peak) and minimum intensity (intensity at 18° 2θ, attributed to amorphous material) to the maximum intensity.

Even though the Segal method is known for its simplicity, it is often used incorrectly (Ling et al., 2019). The (1-10/110) peak has sometimes been used as the peak for amorphous material instead of the minimum intensity between the (200) and (1-10/110) peaks. One should also get rid of environmental scattering from the XRD data through subtraction of a blank run

(Ling et al., 2019) to get a more accurate intensity representing the amorphous material at 18° 2θ. Moreover, the Segal method might not be very accurate as the intensity of the region used for amorphous material can be contributed by the overlap of broad peaks resulting from small crystallites and some small peaks as well (French & Cintrón, 2013; Ling et al., 2019).

An XRD study of hemp fibers, Norway spruce, corn stover, filter paper, and avicel cellulose found that cellulose crystallinity varies based on the origin of cellulose. The high content of cellulose (63 g/100 g dry matter) and high crystallinity calculated according to Segal method, in hemp fibers indicated their suitability for use in strong fiber composites (Gusev, 1978). Another study of natural fibers that combined XRD, FTIR spectroscopy, and thermogravimetric analyses indicated that higher crystallinity and larger crystallite size are associated with slow degradation process and increased thermal stability of lignocellulosic fibers (Poletto, Ornaghi, & Zattera, 2014). The effects of chemical treatments on cellulose crystallinity can be measured using XRD. It has been found that mercerization reduces crystallinity and crystal size in native cellulose of high crystallinity (~ 0.80 to 0.95 C.I. from Segal method), while for low crystallinity celluloses (~0.40 C.I. from the Segal method), the reverse occurs (Revol, Dietrich, & Goring, 1987). Liquid ammonia treatment of native cellulose reduced crystallinity at a low temperature (25°C), whereas crystallinity increased at elevated temperatures (130°C or 140°C) (Mittal et al., 2011). It has also been found that crystallinity was continuously increased in cellulose fibers extracted from rice husks after successive treatments-alkali, bleaching, and acid hydrolysis treatment (Johar et al., 2012). The increased crystallinity was ascribed to the progressive removal of amorphous non-cellulosic materials, which was expected to increase the stiffness and rigidity of cellulose fibers. Another study of cotton linter examined the change in cellulose crystallinities during soda, sulfate, and organosol pulping processes (Gümüskaya, Usta, & Kirci, 2003). It was found that crystallinity, crystallite size, and unit cell type of cellulose in cotton linters were

more affected in organosol pulping conditions. It was also found that operating conditions such as temperature and pressure in cooking digester had major effects on cellulose crystalline structure.

Crystallite size is likewise anticipated to affect the physical characteristics of fibers, including elongation, elastic modulus, tensile strength, yield point, abrasion resistance, fiber swelling, moisture content as well as its and chemical reactivity (Hindeleh, 1980). Natural fibers with larger cellulose crystallite sizes have higher thermal stability (Tyler & Wooding 1958). Regenerated cellulose fibers consisting of small crystallites have better extension and tenacity in the wet state than fibers with larger crystallites (Tyler & Wooding 1958). Line broadening in XRD, or wide-angle X-ray scattering, (WAXS) is commonly used to estimate cellulose crystal size through Scherrer's equation $\tau = \frac{K\,\lambda}{\beta\,cos\theta}$ where τ is the crystallite diameter, λ is the wavelength of incident X-ray, θ is the Bragg angle for the reflection of interest, β is the full width at half maximum of the diffraction peak, and K is the Scherrer's constant as illustrated in **Fig. 7c,** exhibiting the XRD spectra of extracted *R. Raetam* cellulose microfibers. The spectrum shows prominent peaks at approximately 15°, 25° and 35°. The value of K is used between 0.8 to 0.9 assuming Gaussian line profiles of XRD and small cubic crystals of uniform size. This value is widely used to estimate cellulose crystal size (Kim et al., 2013). This formula is, however, valid under the assumption that fluctuations or defects in the crystal lattice are not cumulative, such that deviations from ideal average lattice positions do not disrupt the long-range order of the lattice (Rongpipi et al., 2019). XRD has been applied to estimate the crystal size of cellulose in plant fibers such as cotton and wood fibers such as Norway spruce (Abidi & Manike, 2018; Andersson, Serimaa, Paakkari, Saranpää, & Pesonen, 2003). Like in the case of crystallinity, the mercerization of high crystallinity native cellulose reduced crystallite size, while for low crystallinity celluloses, the reverse trend was observed (Revol et al., 1987). This observation supported the hypothesis that cellulose II

formed from mercerization involves the destruction of cellulose I structure through the separation of the molecular chains. Crystallite size has also been found to change during the soda, sulfate, and organosolv pulping processes of a cotton linter. It was higher in organosolv pulping than in soda and sulfate pulping (Gümüskaya et al., 2003). The effects of heat treatments (oven-dried and moist) on cellulose crystal width in powdered cellulose and two types of wood cellulose (buna and spruce) were measured by XRD techniques (Bhuiyan, Hirai, & Sobue, 2000). It was found that crystal width increased by almost a factor of two after the heat treatment of spruce and buna under moist conditions, whereas it remained almost the same under both conditions in cellulose powder. The increase in crystal width was attributed to rearrangement or reorientation of cellulose molecules in quasi-crystalline parts of amorphous regions. Apart from XRD, small-angle X-ray scattering (SAXS) has also been used to determine the diameter of highly oriented cellulose fibers in ramie, cotton, jute, flax, and Cordura using Guinier plots for cylindrical particles (Heyn, 1955). The values obtained agreed with crystal widths obtained from XRD and electron microscopy. Cellulose crystallite or fiber orientation impacts the physical properties of fibers. Increased orientation causes increased tensile strength and decreased extensibility (Heyn, 1955; Ingersoll, 1946). Crystallite orientation is more strongly correlated with physical properties such as tenacity, stiffness, and elongation, as compared to crystallinity in native Egyptian cotton fibers (Hindeleh, 1980). XRD has been used to study cellulose crystallite orientation through observation of intensity of (002) or (040) reflection at various angles to the fiber axis (Radhakrishnan, Patil, & Dweltz, 1969). Intensity distribution of cellulose (110/020) reflection in regenerated fibers (shown in **Fig. 7d),** known to have cellulose II structure, is often used to characterize the preferred orientation of cellulose crystallites. , The degree of orientation, have also been determined for cellulose fibers from Wide-angle X-ray scattering (WAXS) through Herman's orientation factor f_c calculated as, $f_c = \frac{(3<cos^2\phi> -1)}{2}$ where $<$

$cos^2\phi >$ is the orientation factor, numerically calculated from the WAXS pattern as $< cos^2\phi > = \frac{\int_0^{\pi/2} I(\phi) cos^2\phi sin\phi d\phi}{\int_0^{\pi/2} I(\phi) sin\phi d\phi}$ where ϕ represents the azimuthal angle and I(ϕ) is the intensity along with the (110)/(020) reflection. A maximum orientation parallel to the fiber direction is found when f_c=1, whereas f_c=0 indicates random orientation. Herman's orientation factor has been used to characterize crystallite orientation in regenerated cellulose fibers in an unstrained condition, under tensile strain, and in bending (Gindl, Martinschitz, Boesecke, & Keckes, 2006; Jiang et al., 2012). It has also been found that the degree of orientation was homogeneous in unstrained fiber while it increased linearly with increasing tensile strain applied. In bending, f_c increased in tension and decreased in compression. An XRD study of acid-treated coir fibers found that orientation decreased after acid treatment, which correlated with decreased tenacity and elongation-at-break. Synchrotron-based high spatial resolution WAXS and XRD have examined fiber cellulose crystallite orientation in lyocell and flax fibers (Gindl-Altmutter, Eichhorn, Burghammer, & Keckes, 2014; Kölln et al., 2005). *In situ* tensile tests on single flax fibers with highly oriented cellulose microfibrils found that microfibril orientation improved with increasing strain (C. Baley, 2019). Cellulose microfibril orientation also impacts the mechanical properties of woods. It is often characterized by a parameter called microfibril angle (MFA) defined as the angle made by cellulose microfibrils with the long axis of the cell. MFA has a substantial impact on tensile strength, stiffness, and shrinkage (Kölln et al., 2005)(Altaner & Jarvis, 2008; Cave, 1968). MFA is acquired from XRD via the azimuthal distribution of the cellulose (200) equatorial reflection under the assumption that the cellulose crystals do not have a preferred orientation around the microfibril axis (Cave, 1968; Rongpipi et al., 2019). MFA is also obtained from the streaks in anisotropic SAXS patterns for highly oriented cellulose microfibrils in woody cell walls (Jakob, Fratzl, & Tschegg, 1994; Reiterer, Jakob, Stanzl-Tschegg, & Fratzl, 1998). More recently, a study using grazing incidence wide-angle X-ray scattering (GIWAXS) has

reported that cellulose crystals have preferred orientation with respect to cell wall plane in primary cell walls of onion epidermis, hypocotyls of Arabidopsis thaliana, and moss leaves (Reiterer et al., 1998). The findings of the study contradict a predominant hypothesis of twisting cellulose crystals in primary cell walls. The preferential orientation of cellulose crystals in cell walls could be an important determinant of cell wall growth and biomechanics. Thus, XRD has been very useful in correlating cellulose crystalline structure and properties with natural and chemically treated fiber's physical properties. XRD has been established as the routine method for estimating the crystallinity of cellulose fibers. One should, however, be careful as different XRD methods use different data analysis approaches. Therefore, it is not appropriate to compare cellulose crystallinity indices of samples obtained from different XRD techniques or other analytical techniques as they are not absolute crystallinities. They are useful for comparison only relative to similar samples and only within the same method (Ahvenainen et al., 2016; Park et al., 2010; Rongpipi et al., 2019).

3.2 FOURIER TRANSFORM INFRARED SPECTROSCOPY AND RAMAN SPECTROSCOPY

Raman and FTIR spectroscopy are the two analytical techniques most widely used to elucidate the chemical structure and composition of cellulose fibers. Raman spectroscopy assesses the frequencies at which the sample scatters infrared radiation, whereas IR spectroscopy measures the frequencies at which a sample absorbs radiation. Raman and FTIR spectroscopy are the two most widely used analytical techniques used to elucidate the chemical structure and composition of cellulose fibers. They have been used to analyze various properties, such as the degradability and crystallinity of cellulose and its derivatives (Agarwal, 2014). Both the instrumental techniques are important, as they are sensitive to the structural changes in the materials (Agarwal, 2014; Hospodarova, Singovszka, & Stevulova, 2018; Kavkler & Demšar, 2012; Xia, Xu, Li, Zhang, & Fan,

2019). FTIR, a non-destructive and rapid method, provides information about functional groups present in the molecule (Kruer-Zerhusen, Cantero-Tubilla, & Wilson, 2018; Xu, Yu, Tesso, Dowell, & Wang, 2013). It can also quantify covalent and non-covalent interactions in cellulose. The spectra help to monitor changes in biomass structures due to various physical and chemical treatments (Lupoi, Singh, Simmons, & Henry, 2014). **Fig. 8 a, b** exhibits the FTIR spectra for wood fibers and vegetable fibers, respectively from various sources. A strong broad band at around 3400 cm−1 , is allocated to O–H stretching, the two bands at around 2920 and 2850 cm−1 , are accredited to asymmetric and symmetric methyl and methylene stretching groups present as fiber components. In the fingerprint region, the bands at 1595, 1510 and 1270 cm−1 are assigned to C=C, C–O stretching or bending of various groups present in lignin. The bands at 1460, 1425, 1335, 1220 and 1110 cm^{-1} are typical of C–H, C–O vibrations present in lignin and other carbohydrates. The bands at 1735, 1375, 1240, 1165, 1060 and 1030 cm^{-1} are assigned to C=O, C–H, C–O–C and C–O deformation or stretching vibrations of different groups in carbohydrates.

Raman spectroscopy is another widely used technique for the characterization of cellulose. Here, the specimen is first irradiated with monochromatic laser light of a specific wavelength. A non-elastic spectrum of light results in scattering from the specimen. Raman spectroscopy provides basic information about the vibrations of molecules and the specimen's surface (Cao, Shen, Lu, & Huang, 2006; Edwards, Farwell, & Webster, 1997). Raman spectra of cellulose can be divided into two regions for analysis. The region below 700 cm-1 is sensitive to the cellulose backbone conformation, and the region above 2700 cm-1 is sensitive to hydrogen bonding (Szymańska-Chargot, Cybulska, & Zdunek, 2011; Yan et al., 2008). The Raman spectroscopy has been extensively used in the study of different kinds of plant tissues as it can provide in-depth information on the composition

and structure of various cellular components. IR-FT-RS (Infrared-Fourier Transform-Raman Spectroscopy), a more recent technique differs from conventional Raman spectroscopy in two ways- (i) it is in the near IR range where the laser wavelength used for excitation is, and (ii) a Michelson interferometer is used for the analysis of the scattered light which increases the signal to noise ratio (Agarwal, 2014). Another advantage of Raman spectroscopy is that it provides high spectral resolution with minimal sample preparation. The presence of water in the sample also does not incur any problem in the analysis process (Lupoi et al., 2014). Besides, Raman spectroscopy provides information on the qualitative and quantitative aspects of cellulose or its derivatives (Agarwal, 1986). In an exciting study, micro-Raman spectroscopy was used to study the aging of cellulose fibers from historical objects. The obtained Raman spectra were compared to the spectra of modern cellulose from a database that was created. The Raman spectra of historical cotton showed no luminescence effects, like modern cotton. However, the Raman spectra of historical flax fibers showed prominent luminescence and variations in spectra caused due to degradation. Hence, Raman spectroscopy is an essential tool for identifying cellulose fibers from different sources and for studying their degradation with time (Kavkler & Demšar, 2011). Further, Raman spectroscopy can characterize the chemical structure of cellulose fibers, their crystallinity, and polymorphism (Agarwal, 2017). **Fig 9 a, b, and c** represents the differences in the molecular conformational between cellulose I, cellulose II, and cellulose III. Cellulose spectral information is similar for cellulose II and cellulose III and differs from the spectral information of cellulose I. **Fig 9 d** shows that wood contains less cellulose and more lignin. However, there was no difference between the cellulose crystallinity of compression-wood and normal-wood. The spectra in **Fig 9 e** both showed characteristic bands from cellulose. The major features of the cotton and rayon fiber are very similar in the two spectra. The major difference can be seen in the Raman spectrum at

peak 650 cm^{-1} (C-S-C stretch) which is absent in cotton. FT-IR and Raman microscopy have high potential to explore structure-function relationships, biological processes, and technical treatments as it is possible to reveal cellulose chemistry and structure non-destructively in context with the microstructure.

3.3 NUCLEAR MAGNETIC RESONANCE SPECTROSCOPY

NMR spectroscopy is based on the absorption of electromagnetic radiation by the nuclei of atoms. In NMR, usually, homogenous liquid samples provide sharp signal peaks for quantitative analysis. Since cellulose is insoluble in water or organic solvents, several approaches are used to dissolve, such as acid or enzymatic degradation, or breaking the strong hydrogen bonds (Lindman, Karlström, & Stigsson, 2010). High-resolution magnetic resonance spectrometry, particularly solid-state l3C-NMR spectrometry provides details on chemical environment and ultrastructure besides chemical composition. However, 1H NMR spectroscopy is not preferred compared to 13C spectroscopy. It induces very broad, mutually overlapping signals by enhanced dipolar interaction due to staggered isotropic molecular motion, especially within a polymer (Nehls, Wagenknecht, Philipp, & Stscherbina, 1994). 13C-NMR spectroscopy of pure cellulose shows signals in the region of 60-110 ppm. The peak at 105.5 ppm corresponds to C1, a doublet at 85 and 89 ppm to C4 of crystalline cellulose, 75.5 ppm corresponds to C5, 73.4, and 72.6 ppm relates to C2 or C3 and 65.7 ppm to C6 of cellulose, respectively (Luo et al., 2018). Cross-Polarization Magic Angle Spinning (CP/MAS) 13C NMR analysis of cellulose from birch pulp, cotton linters, and Cladophora sp. was conducted (Shak, Pang, & Mah, 2018). The most informative region in the NMR spectrum was the signal cluster between 80 and 92 ppm that corresponds to C-4. The doublet C4 peaks at 85 and 89 ppm are attributed to signals of C4 atoms on the surface and in the interior of microfibrils, designated as sC4 and iC4, respectively. The assignment of surface and interior atoms was done using density functional theory (DFT) methods and classical

molecular dynamics simulations. The C-4 carbons are disordered, distributed in broadband ranging from 80 to 86 ppm. Synthesis of the nanocrystals from cellulosic fibers involves acid destruction. The acid penetrates cellulose fibers cleaving the glycosidic bonds. Cellulose nanocrystals have many advantages over native cellulose, such as nanoscale size, less toxicity, and high surface area (Shak, et al., 2018). Cellulose nanocrystal was prepared by hydrolysis of cellulose fibers with sulphuric acid has been characterized using the NMR technique (Foston, Hubbell, & Ragauskas, 2011). **Fig. 10 a** shows the spectrum of CNC of sugarcane peel. NMR spectra clarify that most of the carbohydrates disintegrate during acid hydrolysis. The peak observed at 102 ppm, due to hemicellulose, disappears in acid treatment, indicating the removal of hemicellulose. The absence of a peak at 85 ppm of C4 (surface exposed) indicates in-depth penetration of acid into the amorphous structure during hydrolysis of sugarcane. Conclusively all the peaks were due to six carbon atoms of cellulose. The disappearance of several signals also indicated the disruption and leaching of the amorphous region during acid hydrolysis (Foston et al., 2011). Age and time affect the properties of cellulose. It is essential to study such changes while recycling cotton textiles. A survey was conducted to investigate ultrastructural and chemical changes in the cellulose present in cotton sheets using solid-state NMR spectra after a long time of use. It was seen that ss-NMR could detect the effects. The amorphous part of the C4 region (peaks at 85 ppm) of CP/MAS 13C-NMR of the cotton cellulose samples was superimposed where a clear decrease in the signal of the amorphous region can be observed in the sheets that have been washed and laundered compared to the fresh sheets. The C4 region's spectra also conclude that this decrease in signal originates due to the loss of material caused by the leaching of shorter amorphous cellulose chains from the surface. The sheets laundered more than 2–4 times showed only a minor decrease in unstructured signals compared to the former (Parfondry & Perlin, 1977). Similarly, numerous research has been performed to higher

apprehend the ultrastructural changes taking place throughout cellulose isolation. Another application of NMR is to find the purity of the compounds. Using 13C CP/MAS NMR, it was apparent that acid hydrolysis brought on the increase in crystallinity by approximately 10% Populus holocellulose. Microcrystalline cellulose (MCC) was used as a model cellulose substrate because of its highly crystalline nature, making it ideal for analyzing potential alterations occurring in isolated cellulose during holocellulose pulping and the acidic hemicellulose extraction treatment (Richards, Baker, & Iwuoha, 2012) **Fig. 10 c**. Derivatized celluloses or substituted celluloses, such as methylcellulose (MC), hydroxypropyl methylcellulose (HPMC), or carboxymethylcellulose, are important in the pharmaceutical industries for tablet matrices. 13C-NMR spectra of carboxymethylcellulose have been examined to study the properties of substituted cellulose. A peak at 105 ppm corresponding to C-1 was not detected, which shows that the hydrolysis was virtually complete. Moreover, the peaks at the 80-86 ppm region indicate substitution at the 2- and 3- positions of the cellulose. A reasonably sharp peak at 70 ppm was accredited to C-6 atoms with an ether substituent, and this validates the fact that the signal attributable to CH2-6 is of similar intensity. These signals indicate once again that the extent of carboxymethylation at C-6 is intermediate between that at C-2 and C-3 (Hirata & Nishimoto, 1991) which has been depicted in **Fig. 10 b**. NMR has been used to quantify and determine cellulose crystallinity in blended textiles and to study the change of crystallinity in cellulose with age. It has been used to study the ultrastructure of regenerated cellulose to amorphous, crystalline, and para-crystalline cellulose proportions. It also helps to elucidate and understand the influences of physical processing or chemical modification through chemical shifts or changes in peak intensities. NMR studies revealed that cellulose crystallinity is not affected by acid hydrolysis but only results in the fast removal of amorphous cellulose near the cellulose microfibrils surface.

Thus, vibrational spectroscopy techniques are non-destructive method for obtaining the molecular fingerprint of cellulose from various sources in their native or processed state. A combination of vibrational spectroscopy and NMR can provide a complete chemical characterization of cellulose.

3.4 THERMOANALYTICAL TECHNIQUES

Thermal analysis of cellulose is essential for developing various useful products, including fire retardants, paper, and biofilms. Differential scanning calorimetry (DSC) is a thermoanalytical approach wherein the difference in the quantity of heat required to increase the temperature of a sample concerning a reference is measured as a characteristic of temperature (Chakraborty et al., 2021). Similarly, thermogravimetric analysis (TGA) is another analytical technique that monitors the weight change that occurs as a sample is heated at a constant rate. DSC and TGA are used to study the thermal stability of native and processed/ modified cellulose.

3.4.1 DIFFERENTIAL SCANNING CALORIMETRY (DSC)

DSC is the most widely used analytical tool to study cellulose's thermal properties. The increment in temperature and heat flow induces "phase transitions" and provides information about chemical and physical changes such as exothermic and endothermic (Awal et al., 2010). DSC analysis of raw or native cellulose shows an endothermic peak (Lindman et al., 2010) and undertakes a second-order phase transition. A change in endotherms denotes the transition from an initial glassy state to an elastic state (glass transition) (Luo et al., 2018; Wickholm, Larsson, & Iversen, 1998). A characteristic typical endothermic peak in the DSC curve of maize straw cellulose between 250 until 380 °C that was attributed to its thermal decomposition. This peak also has a maximum peak at 342 °C (Miranda, Bica, Nachtigall, Rehman, & Rosa, 2013).

It has been observed that the low crystallinity of the cellulose results in lower thermal

stability (Cho, 2007). Most cellulosic materials consist of crystalline and amorphous regions, and this composition varies depending on the source and origin. The endothermic peaks observed in DSC analysis for native cellulose are usually between 50-150 °C. These endothermic peaks are directly linear with the percentage composition of the amorphous and crystalline cellulose components. The effect on the structural features of amorphous cellulose due to dehydration was also assessed by DSC (Awal et al., 2010). The DSC curve of native cellulose usually shows three distinct regions- first, evaporation of absorbed water (endothermic peak), second decomposition of hemicellulose, depolymerization of cellulose (endothermic peak), and third decomposition of lignin components and α- cellulose (exothermic peak) (Hirata & Nishimoto, 1991). Powdered rice husk samples of Mushkbudij, SR1 and P10 were used to obtain cellulose and nanocellulose. **Fig.11 b** exhibits DSC endotherm of rice husk cellulose and nanocellulose. Raw cellulose fibers are highly integrated with hemicellulose, decreasing their crystallinity, and accelerating thermal degradation (Deepa et al., 2011). It is also known that hemicellulose degrades way before lignin or cellulose due to constituent acetyl groups. Collected cellulose from wheat straw was first acid-treated, followed by DSC analysis. Three distinct regions were mentioned before-two endothermic peaks and one exothermic peak. It was observed that acid-modified cellulose does not entirely degrade and become charred at high temperatures (e.g., 400°C), making it ideal for elevated temperature applications (Huntley, Crews, & Curry, 2015). DSC is also used to study the purity of cellulose and cellulose nanocrystals obtained from different plant sources such as rachis, rubberwood, corn husk, rice husk, macrophyte, banana peels, and jute. CNCs were extracted from the non-edible parts of jackfruit, where a sharp endothermal peak was recorded at 323.5 °C, which is characteristic of cellulose nanocrystals and no peaks corresponding to the hemicellulose and lignin were noted. This is due to the acid treatment which removes the hemicellulose and lignin surrounding cellulose,

making fibrils highly crystalline and resulting in a higher enthalpy. This indicates that acid-treated fibers can withstand extreme heat and processing conditions (Deepa et al., 2011; Trilokesh & Uppuluri, 2019). **Fig 11a** shows the DSC endotherm of cellulose extracted from jackfruit peels. A typical sharp endothermal peak was observed but no peaks for hemicellulose were seen (Trilokesh & Uppuluri, 2019).

Another application of DSC is to study the crystallinity of cellulose. Increasing temperatures disrupt the crystalline domains of cellulose, accompanied by a decrease in the endothermic peak area and the peak temperatures. A higher endothermic activity has been reported in cotton fiber than wood-pulp papers, indicating higher crystallinity of cotton cellulose than wood-pulp cellulose. Because a direct relationship exists between the area of the endothermic peak and the crystallinity of the sample, the cellulose accessibility determines the rate of cellulose hydrolysis by different agents.

Similar to DSC, differential thermal analysis (DTA) is another thermoanlytical technique in which the difference between the sample temperature and the reference temperature at identical heat conditions. Kenaf bast cellulose nano fibrillated fiber (CNF) were analysed using DTA. The DTA curve of unbleached native pulp exhibits two steps of degradation, which was assigned to the hemicellulose and lignin present in the unbleached pulp. The peak temperature of the DTA curve shifted to higher temperatures, thus indicating higher thermal stability (Rizal et al., 2021).

3.4.2 THERMOGRAVIMETRIC ANALYSIS (TGA)

TGA is also used to examine the thermal stability of cellulose. The TGA weight loss curve of native cellulose shows three stages of thermal degradation. The weight loss below 100 °C is due to the evaporation of adsorbed moisture. The second stage (300-360 °C) is assigned to the decomposition of cellulose derivatives, e.g., hemicellulose. The third stage (360-585 °C) may be due to the dissolution of cellulose and oxidation of volatile products and charred residues (Dahiya & Rana,

2004). However, the peak due to absorbed moisture is absent in acid hydrolyzed cellulose (Deepa et al., 2011). Thermal differential simultaneous analysis (simultaneous DSC–TGA) is a technique where samples are simultaneously analyzed using both TGA and DSC techniques. This was used to characterize celluloses from maize straw. Miranda et al., 2013, conducted the thermal stability of cellulose from maize straw using TGA. An initial mass loss of about 4.8 wt% occurs due to water loss and was observed between 30 to 150 °C. The mass loss curve also indicates that cellulose decomposes in a single step in a nitrogen atmosphere at 339 °C as displayed at the maximum of the peak. This also concludes that hemicelluloses and lignin were absent in the isolated cellulose as the characteristic second peak is missing (Miranda, et al., 2013). TGA of cellulose fibers from wood pulp fibers and recycled paper fibers was studied and differences in their thermal decomposition and weight loss were observed. These differences are due to different cellulose contents in the fibers and the presence of impurities, such as CaCO3 used as fillers in papers. The observed first mass loss is due to the initial dehydration, where 0.55 – 1.22 % of water is evaporated in the temperature range of 25 °C and 127 °C. The second and highest decrease in weight of the cellulosic fibers was seen at 206-400 °C suggesting the decomposition of amorphous cellulose. The depolymerization of hemicellulose occurs between 180-350 °C. The random cleavage in the glycosidic linkage of cellulose occurs between 275-350 °C and the decomposition of residual lignin starts at 160 °C and completes at 900 °C (Ševulova, Hospodárova, & Eštoková, 2017). **Fig 11 c, d** exhibits TGA analysis performed on the Greencel wood pulp fibres with varying cellulose contents and rice rusk respectively. Cellulose is a long polymer of glucose monomers where the crystalline regions of the granules contribute to its thermal stability (Poletto et al., 2014). The higher onset of degradation temperatures indicates the improved thermal stability of the material. Cellulose nanofibers of diameters among 10–80 nm have been extracted from wheat straw. TGA was used to study the thermal stability of these fibers and it was determined that the degradation temperature was accelerated after each step of the isolation process as exhibited in **fig 11 e**. However, 3 tiers of

decay have been found in TGA curves. The preliminary weight reduction of fibers (100–150 °C) is because of the moisture evaporation. The maximum weight reduction occurred between 250–350 °C. The final stage of decomposition is because of the decomposition of the fiber components. The higher onset of decay temperatures refers to improved thermal stability. These results indicate that wheat straw fiber's thermal stability increases post chemical treatments (Alemdar & Sain, 2008).

3.5 SURFACE CHARACTERIZATION THROUGH WATER CONTACT ANGLE

The contact angle is used to study the wettability of cellulose and cellulose-based products which in turn affects their ink receptivity, absorbency, coating, and adhesion, and frictional properties. Further, an increase in hydrophilicity results in anti-fouling properties which can be measured in terms of water contact angle (WCA). While a higher WCA indicates more hydrophobicity, lower values indicate lower hydrophobicity or higher hydrophilicity (Jonoobi, Ashori, & Siracusa, 2019). Cellulose is hydrophilic and swells in the occurrence of water and measuring the WCA is unfeasible because of the instant water infiltration. However, in cellulose treated with plasma, the contact angle was determined to be 145°, indicating increased hydrophobic (Singh, Kaushik, & Ahuja, 2016). Recently, microfibrillated aggregates of cellulose (MFCs) and nanofibrillated cellulose (NFCs) were extracted from wheat straw and subjected to propionylation under different processing conditions of time, temperature, and concentration. The hydrophobicity increased due to propionylation as the WCA increased up to 121° and 119° for MFCs and NFCs, respectively. However, an increase in reaction time and temperature resulted in a reduction of the contact angle down to 65◦ (Hietala, Varrio, Berglund, Soini, & Oksman, 2018). Cellulose nanofibres (CNFs) were acquired from wastepaper using three different procedures, namely pulping, flotation, and washing. The WCA of the CNF networks fluctuated depending on the used treatment: the flotation-treated networks were turned out to be more hydrophilic (contact angle 52.5°) compared to the hydrophobic washed networks (contact angle 72.6°) (Kolářová, Vosmanská, Rimpelová, & Švorčík, 2013).

4. CONCLUSION

Currently, the increasing demand for cellulose and its derivatives in various fields has created a need for further in-depth study and characterization using novel biophysical techniques to further understand the properties of cellulose. These modified forms of cellulose differ in terms of their properties from each other and their native forms. Hence, there is a dire need to characterize cellulose in its native and modified form. A wide variety of microscopy techniques including optical microscopy, nonlinear optical microscopy, electron microscopy, and atomic force microscopy have been used to study the detailed morphology and ultrastructure of cellulose. Further, X-ray diffraction, vibrational spectroscopy, and thermoanalytical techniques have been used to reveal the physicochemical and functional properties of cellulose. Light microscopy is non-invasive, economical, and immediate and can be used for preliminary observation of cellulose. However, it can be employed only in the presence of light and provides low resolution. Further, nonlinear optical methods have the advantages of deep sample penetration, great sensitivity, and ultrahigh resolution. On the other hand, although SEM provided high resolution, they are expensive with complex sample preparation. Compared to SEM, TEM provides information about internal structures, making it extremely efficient. In addition, AFM can produce a three-dimensional topography and provides superior details of surfaces, compared to SEM which cannot resolve the faint variations on an extremely smooth surface. Further, AFM also confirms the variations in mechanical and chemical properties of cellulose thus helps in validating the result obtained from other techniques like IR spectroscopy.

Other techniques like XRD are used to measure crystalline. However, small crystalline structures might go undetected by the X-rays resulting in inappropriate results. A massive advantage of using Raman spectroscopy over infrared spectroscopy is easy sample

preparation. On the contrary, IR spectroscopy is much more cost effective and sensitive compared to Raman spectroscopy which utilises high powered lasers. Thermoanalytical techniques like DSC and TGA can be used to study the transition temperature, thermal stability and purity of cellulose using very little sample. However, these techniques are destructive and cannot analyse heterogenous materials. Thus, morphological, chemical, and structural characterization of cellulose using advanced, yet convenient techniques contribute highly to the study and understanding of various crucial aspects including the formation of nano cellulose, mechanism of acid and enzymatic degradation, cellulose modifications, and thermal degradations. These parameters are key factors to be considered while using cellulose as a raw material.

Conflicts of interest

The authors declare no conflict of interest.

Acknowledgment

We thank the Department of Biotechnology (DBT) and Department of Science and Technology (DST), Government of India, for the financial support (project number: BT/PR25099/NER/95/1014/2017 and DST/INT/BLG/P-03/2019). NM thank Manipal Academy of Higher Education (MAHE), Manipal and Technology Information Forecasting and Assessment Council-Centre of Relevance and Excellence (TIFAC-CORE) in Pharmacogenomics, Manipal School of Life Sciences, MAHE for providing the infrastructure and facilities. IC thank MAHE, Manipal, Karnataka, India for the Dr. T.M.A. Pai Ph.D. fellowship. SR, EWG, and EDG acknowledge support as part of the Center for Lignocellulose Structure and Formation, an Energy Frontier Research Center funded by the US Department of Energy, Office of Science, Basic Energy Sciences under award no. DE-SC0001090.

REFERENCES

Abidi, N., & Manike, M. (2018). X-ray diffraction and FTIR investigations of cellulose deposition during cotton fiber development. *Textile Research Journal*, 88, 719-730. https://doi.org/10.1177/0040517516688634

Abiaziem, C.V., Williams, A.B., Inegbenebor, A.I., Onwordi, C.T., Ehi-Eromosele, C.O. and Petrik, L.F., (2019), August. Adsorption of lead ion from aqueous solution unto cellulose nanocrystal from cassava peel. In *Journal of Physics: Conference Series* (Vol. 1299, No. 1, p. 012122). IOP Publishing.

Agarwal, U. P. (2014). 1064 nm FT-Raman spectroscopy for investigations of plant cell walls and other biomass materials. *Frontiers in Plant Science*, 5, 490. https://doi.org/10.3389/fpls.2014.00490

Agarwal, U. P. (2017). Raman spectroscopy in the analysis of cellulose nanomaterials. In Nanocelluloses: Their Preparation, Properties, and Applications. *American Chemical Society*, pp. 75-90.

Ahvenainen, P., Kontro, I., & Svedström, K. (2016). Comparison of sample crystallinity determination methods by X-ray diffraction for challenging cellulose I materials. *Cellulose*, 23, 1073-1086. https://doi.org/10.1007/s10570-016-0881-6

Alemdar, A., & Sain, M. (2008). Biocomposites from wheat straw nanofibers: Morphology, thermal and mechanical properties. *Composites Science and Technology,* 68, 557-565. https://doi.org/10.1016/j.compscitech.2007.05.044

Altaner, C. M., & Jarvis, M. C. (2008). Modelling polymer interactions of the 'molecular Velcro'type in wood under mechanical stress. *Journal of Theoretical Biology,* 253, 434-445. https://doi.org/10.1016/j.jtbi.2008.03.010

Andersson, S., Serimaa, R., Paakkari, T., Saranpää, P., & Pesonen, E. (2003). Crystallinity of wood and the size of cellulose crystallites in Norway spruce (Picea abies). *Journal of Wood Science*, 49, 531-537. https://doi.org/10.1007/s10086-003-0518-x

Atalla, R. H., & Nagel, S. C. (1974). Annealing and increased order in cellulose II. *Journal of Polymer Science: Polymer Letters Edition*, 12, 565-568. https://doi.org/10.1002/pol.1974.130121005

Awal, A., Ghosh, S., & Sain, M. (2010). Thermal properties and spectral characterization of wood pulp reinforced bio-composite fibers. *Journal of Thermal Analysis and Calorimetry*, 99, 695-701. https://doi.org/10.1007/s10973-009-0100-x

Baker, A. A., Helbert, W., Sugiyama, J., & Miles, M. J. (1997). High-resolution atomic force microscopy of nativeValoniacellulose I microcrystals. *Journal of Structural Biology*, 119, 129-138. https://doi.org/10.1006/jsbi.1997.3866

Baker, A.A., Helbert, W., Sugiyama, J. and Miles, M.J., 1997. High-resolution atomic force microscopy of native Valoniacellulose I microcrystals. *Journal of Structural Biology*, 119,129-138.

Baker, A. A., Helbert, W., Sugiyama, J., & Miles, M. J. (2000). New insight into cellulose structure by atomic force microscopy shows the Iα crystal phase at near-atomic resolution. *Biophysical Journal*, 79, 1139-1145. https://doi.org/10.1016/S0006-3495(00)76367-3

Baley, C. (2002). Analysis of the flax fibres tensile behaviour and analysis of the tensile stiffness increase. *Composites Part A: Applied Science and Manufacturing,* 33, 939-948. https://doi.org/10.1016/S1359-835X(02)00040-4

Baley, C., Perrot, Y., Busnel, F., Guezenoc, H., & Davies, P. (2006). Transverse tensile behaviour of unidirectional plies reinforced with flax fibres. *Materials Letters,* 60, 2984-2987. https://doi.org/10.1016/j.matlet.2006.02.028

Balnois, E., Busnel, F., Baley, C., & Grohens, Y. (2007). An AFM study of the effect of chemical treatments on the surface microstructure and adhesion properties of flax fibres. *Composite Interfaces*, 14, 715-731. https://doi.org/10.1163/156855407782106537

Bastidas, J. C., Venditti, R., Pawlak, J., Gilbert, R., Zauscher, S., & Kadla, J. F. (2005). Chemical force microscopy of cellulosic fibers. *Carbohydrate Polymers*, 62, 369-378. https://doi.org/10.1016/j.carbpol.2005.08.058

Beyene, D., Chae, M., Dai, J., Danumah, C., Tosto, F., Demesa, A. G., & Bressler, D. C. (2018). Characterization of cellulase-treated fibers and resulting cellulose nanocrystals generated through acid hydrolysis. *Materials,* 11, 1272. https://doi.org/10.3390/ma11081272

Bhuiyan, M. T. R., Hirai, N., & Sobue, N. (2000). Changes of crystallinity in wood cellulose by heat treatment under dried and moist conditions. *Journal of Wood Science*, 46, 431-436. https://doi.org/10.1007/BF00765800

Bunaciu, A. A., UdriŞTioiu, E. G., & Aboul-Enein, H. Y. (2015). X-ray diffraction: instrumentation and applications. *Critical reviews in Analytical Chemistry*, 45, 289-299. https://doi.org/10.1080/10408347.2014.949616

Cao, Y., Shen, D., Lu, Y., & Huang, Y. (2006). A Raman-scattering study on the net orientation of biomacromolecules in the outer epidermal walls of mature wheat stems (Triticum aestivum). *Annals of Botany*, 97, 1091-1094. https://doi.org/10.1093/aob/mcl059

Cave, I. D. (1968). The anisotropic elasticity of the plant cell wall. *Wood science and technology*, 2, 268-278. https://doi.org/10.1007/BF00350273

Chakraborty, I., Pallen, S., Shetty, Y., Roy, N., & Mazumder, N. (2020). Advanced microscopy techniques for revealing molecular structure of starch granules. *Biophysical Reviews*, 12(1), 105-122. https://doi.org/10.1007/s12551-020-00614-7

Chakraborty, I., Govindaraju, I., Rongpipi, S., Mahato, K. K., & Mazumder, N. (2021). Effects of Hydrothermal Treatments on Physicochemical Properties and In Vitro Digestion of Starch. *Food Biophysics*, 1-11. https://doi.org/10.1007/s11483-021-09687-7

Chandra, J., George, N., & Narayanankutty, S. K. (2016). Isolation and characterization of cellulose nanofibrils from arecanut husk fibre. *Carbohydrate Polymers,* 142, 158-166. https://doi.org/10.1016/j.carbpol.2016.01.015

Chary, K. V. R., & Srivastava, A. K. (2013). Encyclopedia of Biophysics. *Encyclopedia of Biophysics* doi:10.1007/978-3-642-16712-6.

Cherian, B. M., Leão, A. L., De Souza, S. F., Thomas, S., Pothan, L. A., & Kottaisamy, M. (2010). Isolation of nanocellulose from pineapple leaf fibres by steam explosion. *Carbohydrate Polymers,* 81, 720-725. https://doi.org/10.1016/j.carbpol.2010.03.046

Chinga-Carrasco, G., & Syverud, K. (2010). Computer-assisted quantification of the multi-scale structure of films made of nanofibrillated cellulose. *Journal of Nanoparticle Research*, 12, 841-851. https://doi.org/10.1007/s11051-009-9710-2

Cho, L. (2007). Identification of textil fiber by Raman microspectroscopy. *Forensic Science Journal*, *1*, 55–62.

Choi, M., Kang, Y. R., Lim, I. S., & Chang, Y. H. (2018). Structural characterization of cellulose obtained from extraction wastes of graviola (annona muricata) leaf. *Preventive Nutrition and Food science*, 23, 166 - 170. https://doi.org/10.3746/pnf.2018.23.2.166

Ciolacu, D., Ciolacu, F., & Popa, V. I. (2011). Amorphous cellulose - Structure and characterization. *Cellulose Chemistry and Technology*, *45*(1–2), 13–21.

Dahiya, J. B., & Rana, S. (2004). Thermal degradation and morphological studies on cotton cellulose modified with various arylphosphorodichloridites. *Polymer International*, 53, 995-1002. https://doi.org/10.1002/pi.1500

Deepa, B., Abraham, E., Cherian, B. M., Bismarck, A., Blaker, J. J., Pothan, L. A., ... & Kottaisamy, M. (2011). Structure, morphology and thermal characteristics of banana nano fibers obtained by steam explosion. *Bioresource Technology,* 102, 1988-1997. https://doi.org/10.1016/j.biortech.2010.09.030

Deguchi, S., Tsujii, K., & Horikoshi, K. (2006). Cooking cellulose in hot and compressed water. *Chemical Communications,* 31, 3293-3295. https://doi.org/10.1039/B605812D

Ding, S. Y., Zhao, S., & Zeng, Y. (2014). Size, shape, and arrangement of native cellulose fibrils in maize cell walls. *Cellulose*, 21, 863-871. https://doi.org/10.1007/s10570-013-0147-5

Doh, S.J., Lee, J.Y., Lim, D.Y. and Im, J.N., (2013). Manufacturing and analyses of wet-laid nonwoven consisting of carboxymethyl cellulose fibers. *Fibers and Polymers*, 14, 2176-2184.

Edwards, H. G. M., Farwell, D. W., & Webster, D. (1997). FT Raman microscopy of untreated natural plant fibres. *Spectrochimica Acta Part A: Molecular and Biomolecular Spectroscopy*, 53, 2383-2392. https://doi.org/10.1016/S1386-1425(97)00178-9

Effah, B., Van Reenen, A. and Meincken, M., (2015). Characterisation of the Interfacial Adhesion of the Different Components in Wood–Plastic Composites with AFM. *Springer Science Reviews*, 3, 97-111.

Eronen, P., Österberg, M., & Jääskeläinen, A. S. (2009). Effect of alkaline treatment on cellulose supramolecular structure studied with combined confocal Raman spectroscopy and atomic force microscopy. *Cellulose*, 16, 167-178. https://doi.org/10.1007/s10570-008-9259-8

Fardim, P., Gustafsson, J., Schoultz, S., Peltonen, J., & Holmbom, B. (2005). Extractives on fiber surfaces investigated by XPS, ToF-SIMS and AFM. *Colloids and Surfaces A: Physicochemical and Engineering Aspects,* 255, 91-103. https://doi.org/10.1016/j.colsurfa.2004.12.027

Foston, M. B., Hubbell, C. A., & Ragauskas, A. J. (2011). Cellulose isolation methodology for NMR analysis of cellulose ultrastructure. *Materials,* 4, 1985-2002. https://doi.org/10.3390/ma4111985

Ford, Z.M., Stevens, E.D., Johnson, G.P. and French, A.D., 2005. Determining the crystal structure of cellulose II by modeling. *Carbohydrate Research*, 340, 827-833.

Fratzl, P., & Weinkamer, R. (2007). Nature's hierarchical materials. *Progress in Materials Science,* 52, 1263-1334. https://doi.org/10.1016/j.pmatsci.2007.06.001

French, A. D., & Cintrón, M. S. (2013). Cellulose polymorphy, crystallite size, and the Segal crystallinity index. *Cellulose*, 20, 583-588. https://doi.org/10.1007/s10570-012-9833-y

French, A. D. (2014). Idealized powder diffraction patterns for cellulose polymorphs. *Cellulose,* 21, 885-896. https://doi.org/10.1007/s10570-013-0030-4

Garside, P., & Wyeth, P. (2006). Identification of cellulosic fibres by FTIR spectroscopy differentiation of flax and hemp by polarized ATR FTIR. *Studies in Conservation,* 51, 205-211. https://doi.org/10.1179/sic.2006.51.3.205

Gilli, E., Kappel, L., Hirn, U., & Schennach, R. (2009). An optical model for polarization microscopy analysis of pulp fibre-to-fibre bonds. *Composite Interfaces,* 16, 901-922. https://doi.org/10.1163/092764409X12477474036798

Gindl-Altmutter, W., Eichhorn, S. J., Burghammer, M., & Keckes, J. (2014). Radial crystalline texture in a lyocell fibre revealed by synchrotron nanofocus wide-angle X-ray scattering. *Cellulose,* 21, 845-851. https://doi.org/10.1007/s10570-013-0140-z

Gindl, W., Martinschitz, K. J., Boesecke, P., & Keckes, J. (2006). Orientation of cellulose crystallites in regenerated cellulose fibres under tensile and bending loads. *Cellulose*, 13, 621-627. https://doi.org/10.1007/s10570-006-9074-z

Govindaraju, I., Chakraborty, I., Baruah, V. J., Sarmah, B., Mahato, K. K., & Mazumder, N. (2021). Structure and Morphological Properties of Starch Macromolecule Using

Biophysical Techniques. *Starch - Stärke* , 73, 2000030, 1 - 12. https://doi.org/10.1002/star.202000030

Govindaraju, I., Zhuo, G. Y., Chakraborty, I., Melanthota, S. K., Mal, S. S., Sarmah, B., Baruah, V, J., Mahato, K.K., & Mazumder, N. (2022). Investigation of structural and physico-chemical properties of rice starch with varied amylose content: A combined microscopy, spectroscopy, and thermal study. *Food Hydrocolloids,* 122, 107093. https://doi.org/10.1016/j.foodhyd.2021.107093

Gümüskaya, E., Usta, M., & Kirci, H. (2003). The effects of various pulping conditions on crystalline structure of cellulose in cotton linters. *Polymer Degradation and Stability,* 81, 559-564. https://doi.org/10.1016/S0141-3910(03)00157-5

Gusev, G. V. (1978). Hermans-Weidinger X-ray diffraction technique for determining polymer crystallinity and the use of the Ruland ratio. *Polymer Science USSR*, 20, 1295-1297. https://doi.org/10.1016/0032-3950(78)90270-8

Gustafsson, J., Ciovica, L., & Peltonen, J. (2003). The ultrastructure of spruce kraft pulps studied by atomic force microscopy (AFM) and X-ray photoelectron spectroscopy (XPS). *Polymer*, 44, 661-670. https://doi.org/10.1016/S0032-3861(02)00807-8

Hanley, S. J., Revol, J. F., Godbout, L., & Gray, D. G. (1997). Atomic force microscopy and transmission electron microscopy of cellulose from Micrasterias denticulata; evidence for a chiral helical microfibril twist. *Cellulose,* 4, 209-220. https://doi.org/10.1023/A:1018483722417

Hawinkels, R. J. H., Beex, R. H. J., & Peerlings, E. L. (2009). A microscopic study of cellulosic fibre networks. Eindhoven University of Technology, Department of Mechanical Engineering.

Hellwig, J., Durán, V. L., & Pettersson, T. (2018). Measuring elasticity of wet cellulose fibres with AFM using indentation and a linearized Hertz model. *Analytical Methods,* 10, 3820-3823. https://doi.org/10.1039/C8AY00816G

Henderson, E. (1994). Imaging of living cells by atomic force microscopy. *Progress in Surface Science,* 46, 39-60. https://doi.org/10.1016/0079-6816(94)90006-X

Heyn, A. N. (1955). Small Particle X-Ray Scattering by Fibers, Size and Shape of Microcrystallites. *Journal of Applied Physics*, 26, 519-526. https://doi.org/10.1063/1.1722032

Heyn, A. N. (1969). The elementary fibril and supermolecular structure of cellulose in soft wood fiber. *Journal of Ultrastructure Research*, *26*, 52-68. https://doi.org/10.1016/S0022-5320(69)90035-5

Hietala, M., Varrio, K., Berglund, L., Soini, J., & Oksman, K. (2018). Potential of municipal solid waste paper as raw material for production of cellulose nanofibres. *Waste Management*, 80, 319-326. https://doi.org/10.1016/j.wasman.2018.09.033

Hindeleh, A. M. (1980). Crystallinity, crystallite size, and physical properties of native Egyptian cotton. *Textile Research Journal*, 50, 667-674. https://doi.org/10.1177/004051758005001106

Hirata, T., & Nishimoto, T. (1991). DSC, DTA, and TG of cellulose untreated and treated with flame-retardants. *Thermochimica Acta*, 193, 99-106. https://doi.org/10.1016/0040-6031(91)80177-K

Hoffmann, Á., Jungk, T., & Soergel, E. (2007). Cross-talk correction in atomic force microscopy. *Review of Scientific Instruments*, 78, 016101. https://doi.org/10.1063/1.2424448

Hospodarova, V., Singovszka, E., & Stevulova, N. (2018). Characterization of cellulosic fibers by FTIR spectroscopy for their further implementation to building materials. *American Journal of Analytical Chemistry,* 9, 303-310. https://doi.org/10.4236/ajac.2018.96023

Hosseinali, F., & Thomasson, J. A. (2019). Probing of Nanoscale Friction and Mechanical Characteristics of Cotton Fiber's Surface. *Fibers,* 7, 64. https://doi.org/10.3390/fib7070064

Huntley, C. J., Crews, K. D., & Curry, M. L. (2015). Chemical functionalization and characterization of cellulose extracted from wheat straw using acid hydrolysis methodologies. *International Journal of Polymer Science*, 293981. https://doi.org/10.1155/2015/293981

Ingersoll, H. G. (1946). Fine structure of viscose rayon. *Journal of Applied Physics*, 17, 924-939. https://doi.org/10.1063/1.1707665

Issa, R.M., Abou-Sekkina, M.M., Khedr, A.M., Bastawisy, A.E.D.M. and El-Helece, W.A., (2016). Trace the exploitation of Egyptian rice straw through spectral and thermal measurements. *Arabian Journal of Chemistry*, 9, 130-137.

Ishikawa, A., Okano, T., & Sugiyama, J. (1997). Fine structure and tensile properties of ramie fibres in the crystalline form of cellulose I, II, IIII and IVI. *Polymer*, 38, 463-468. https://doi.org/10.1016/S0032-3861(96)00516-2

Jakob, H. F., Fratzl, P., & Tschegg, S. E. (1994). Size and arrangement of elementary cellulose fibrils in wood cells: a small-angle X-ray scattering study of Picea abies. *Journal of Structural Biology,* 113, 13-22. https://doi.org/10.1006/jsbi.1994.1028

Jenkins, L. M., & Donald, A. M. (1997). Use of the environmental scanning electron microscope for the observation of the swelling behaviour of cellulosic fibres. *Scanning,* 19, 92-97. https://doi.org/10.1002/sca.4950190206

Jiang, G., Huang, W., Li, L., Wang, X., Pang, F., Zhang, Y., & Wang, H. (2012). Structure and properties of regenerated cellulose fibers from different technology processes. *Carbohydrate Polymers,* 87, 2012 - 2018. https://doi.org/10.1016/j.carbpol.2011.10.022

Johar, N., Ahmad, I., & Dufresne, A. (2012). Extraction, preparation and characterization of cellulose fibres and nanocrystals from rice husk. *Industrial Crops and Products,* 37, 93-99. https://doi.org/10.1016/j.indcrop.2011.12.016

Jonoobi, M., Ashori, A., & Siracusa, V. (2019). Characterization and properties of polyethersulfone/modified cellulose nanocrystals nanocomposite membranes. *Polymer Testing,* 76, 333-339. https://doi.org/10.1016/j.polymertesting.2019.03.039

Ju, X., Bowden, M., Brown, E.E. and Zhang, X., (2015). An improved X-ray diffraction method for cellulose crystallinity measurement. *Carbohydrate Polymers*, 123, 476-481.

Kafle, K., Xi, X., Lee, C. M., Tittmann, B. R., Cosgrove, D. J., Park, Y. B., & Kim, S. H. (2014). Cellulose microfibril orientation in onion (Allium cepa L.) epidermis studied by atomic force microscopy (AFM) and vibrational sum frequency generation (SFG) spectroscopy. *Cellulose,* 21, 1075-1086. https://doi.org/10.1007/s10570-013-0121-2

Kalita, E., Nath, B. K., Deb, P., Agan, F., Islam, M. R., & Saikia, K. (2015). High quality fluorescent cellulose nanofibers from endemic rice husk: Isolation and characterization. *Carbohydrate polymers,* 122, 308-313. https://doi.org/10.1016/j.carbpol.2014.12.075

Kalita, R. D., Nath, Y., Ochubiojo, M. E., & Buragohain, A. K. (2013). Extraction and characterization of microcrystalline cellulose from fodder grass; Setaria glauca (L) P. Beauv, and its potential as a drug delivery vehicle for isoniazid, a first line antituberculosis drug. *Colloids and Surfaces B: Biointerfaces,* 108, 85-89. https://doi.org/10.1016/j.colsurfb.2013.02.016

Kaushik, A., & Singh, M. (2011). Isolation and characterization of cellulose nanofibrils from wheat straw using steam explosion coupled with high shear homogenization. *Carbohydrate Research,* 346, 76-85. https://doi.org/10.1016/j.carres.2010.10.020

Kaushik, M., Fraschini, C., Chauve, G., Putaux, J.-L., & Moores, A. (2015). Transmission Electron Microscopy for the Characterization of Cellulose Nanocrystals. *The Transmission Electron Microscope - Theory and Applications*

Kavkler, K., & Demšar, A. (2011). Examination of cellulose textile fibres in historical objects by micro-Raman spectroscopy. *Spectrochimica Acta Part A: Molecular and Biomolecular Spectroscopy*, *78*, 740-746. https://doi.org/10.1016/j.saa.2010.12.006

Kavkler, K., & Demsar, A. (2012). Application of FTIR and Raman spectroscopy to qualitative analysis of structural changes in cellulosic fibres. *Tekstilec*, *55*, 19-31.

Khenblouche, A., Bechki, D., Gouamid, M., Charradi, K., Segni, L., Hadjadj, M. and Boughali, S., (2019). Extraction and characterization of cellulose microfibers from Retama raetam stems. Polímeros, 29.

Kim, S. H., Lee, C. M., & Kafle, K. (2013). Characterization of crystalline cellulose in biomass: Basic principles, applications, and limitations of XRD, NMR, IR, Raman, and SFG. *Korean Journal of Chemical Engineering*, *30*, 2127-2141. https://doi.org/10.1007/s11814-013-0162-0

Kino, G. S., & Corle, T. R. (1996). *Confocal scanning optical microscopy and related imaging systems.* Academic Press.

Kirby, A. R., Gunning, A. P., Waldron, K. W., Morris, V. J., & Ng, A. (1996). Visualization of plant cell walls by atomic force microscopy. *Biophysical Journal*, *70*, 1138-1143. https://doi.org/10.1016/S0006-3495(96)79708-4

Kolářová, K., Vosmanská, V., Rimpelová, S., & Švorčík, V. (2013). Effect of plasma treatment on cellulose fiber. *Cellulose*, *20*, 953-961. https://doi.org/10.1007/s10570-013-9863-0

Kölln, K., Grotkopp, I., Burghammer, M., Roth, S. V., Funari, S. S., Dommach, M., & Müller, M. (2005). Mechanical properties of cellulose fibres and wood. Orientational aspects in situ investigated with synchrotron radiation. *Journal of Synchrotron Radiation*, *12*, 739-744. https://doi.org/10.1107/S0909049505011714

Kontturi, E., Thüne, P. C., Alexeev, A., & Niemantsverdriet, J. W. (2005). Introducing open films of nanosized cellulose—atomic force microscopy and quantification of morphology. *Polymer*, 46, 3307-3317. https://doi.org/10.1016/j.polymer.2005.02.087

Kroon-Batenburg, L.M.J. and Kroon, J., 1997. The crystal and molecular structures of cellulose I and II. *Glycoconjugate Journal*, 14, 677-690.

Kruer-Zerhusen, N., Cantero-Tubilla, B., & Wilson, D. B. (2018). Characterization of cellulose crystallinity after enzymatic treatment using Fourier transform infrared spectroscopy (FTIR). *Cellulose*, *25*, 37-48. https://doi.org/10.1007/s10570-017-1542-0

Kuutti, L., Peltonen, J., Pere, J., & Teleman, O. (1995). Identification and surface structure of crystalline cellulose studied by atomic force microscopy. *Journal of Microscopy*, *178*, 1 - 6. https://doi.org/10.1111/j.1365-2818.1995.tb03573.x

Lai, Y., Zhang, H., Sugano, Y., Xie, H., & Kallio, P. (2019). Correlation of Surface Morphology and Interfacial Adhesive Behavior between Cellulose Surfaces: Quantitative Measurements in Peak-Force Mode with the Colloidal Probe Technique. *Langmuir*, *35*, 7312-7321. https://doi.org/10.1021/acs.langmuir.8b03503

Le Moigne, N., & Navard, P. (2010). Dissolution mechanisms of wood cellulose fibres in NaOH–water. *Cellulose*, *17*, 31-45. https://doi.org/10.1007/s10570-009-9370-5

Lee, I., Evans, B. R., & Woodward, J. (2000). The mechanism of cellulase action on cotton fibers: evidence from atomic force microscopy. *Ultramicroscopy*, *82*, 213-221. https://doi.org/10.1016/S0304-3991(99)00158-8

Lindman, B., Karlström, G., & Stigsson, L. (2010). On the mechanism of dissolution of cellulose. *Journal of Molecular Liquids*, *156*, 76-81. https://doi.org/10.1016/j.molliq.2010.04.016

Ling, Z., Wang, T., Makarem, M., Cintrón, M. S., Cheng, H. N., Kang, X., & French, A. D. (2019). Effects of ball milling on the structure of cotton cellulose. *Cellulose*, *26*, 305-328. https://doi.org/10.1007/s10570-018-02230-x

Luo, M. T., Li, H. L., Huang, C., Zhang, H. R., Xiong, L., Chen, X. F., & Chen, X. D. (2018). Cellulose-based absorbent production from bacterial cellulose and acrylic acid: synthesis and performance. *Polymers*, *10*(7), 702 - 708. https://doi.org/10.3390/polym10070702

Lupoi, J. S., Singh, S., Simmons, B. A., & Henry, R. J. (2014). Assessment of lignocellulosic biomass using analytical spectroscopy: an evolution to high-throughput techniques. *BioEnergy Research*, *7*, 1-23. https://doi.org/10.1007/s12155-013-9352-1

Magonov, S. N., Elings, V., & Whangbo, M. H. (1997). Phase imaging and stiffness in tapping-mode atomic force microscopy. *Surface Science, 375,* 385 - 391. https://doi.org/10.1016/S0039-6028(96)01591-9.

Marinello, F., Bariani, P., Savio, E., Horsewell, A., & De Chiffre, L. (2008). Critical factors in SEM 3D stereo microscopy. *Measurement Science and Technology*, 19, 1 - 12. https://doi.org/10.1088/0957-0233/19/6/065705.

Mazumder, N., Balla, N. K., Zhuo, G. Y., Kistenev, Y. V., Kumar, R., Kao, F. J.,& Krivova, N. A. (2019). Label-free non-linear multimodal optical microscopy—basics, development, and applications. *Frontiers in Physics*, *7*, 170 - 176. https://doi.org/10.3389/fphy.2019.00170

Mazumder, N., Qiu, J., Foreman, M. R., Romero, C. M., Török, P., & Kao, F. J. (2013). Stokes vector based polarization resolved second harmonic microscopy of starch granules. *Biomedical Optics Express*, *4*, 538-547. https://doi.org/10.1364/BOE.4.000538

Miranda, M. I. G., Bica, C. I. D., Nachtigall, S. M. B., Rehman, N., & Rosa, S. M. L. (2013). Kinetical thermal degradation study of maize straw and soybean hull celluloses by simultaneous DSC–TGA and MDSC techniques. *Thermochimica Acta*, *565*, 65-71. https://doi.org/10.1016/j.tca.2013.04.012

Mittal, A., Katahira, R., Himmel, M. E., & Johnson, D. K. (2011). Effects of alkaline or liquid-ammonia treatment on crystalline cellulose: changes in crystalline structure and effects on enzymatic digestibility. *Biotechnology for Biofuels*, *4*, 1-16. https://doi.org/10.1186/1754-6834-4-41

Nehls, I., Wagenknecht, W., Philipp, B., & Stscherbina, D. (1994). Characterization of cellulose and cellulose derivatives in solution by high resolution 13C-NMR spectroscopy. *Progress in Polymer Science,* 19, 29-78. https://doi.org/10.1016/0079-6700(94)90037-X

Nigmatullin, R., Lovitt, R., Wright, C., Linder, M., Nakari-Setälä, T., & Gama, M. (2004). Atomic force microscopy study of cellulose surface interaction controlled by cellulose binding domains. *Colloids and Surfaces B: Biointerfaces*, *35*, 125-135. https://doi.org/10.1016/j.colsurfb.2004.02.013

Noy, A., Vezenov, D. V., & Lieber, C. M. (1997). Chemical force microscopy. *Annual Review of Materials Science*, *27*, 381-421. https://doi.org/10.1146/annurev.matsci.27.1.381

Paiva, A. T., Sequeira, S. M., Evtuguin, D. V., Kholkin, A. L., & Portugal, I. (2007). Nanoscale structure of cellulosic materials: challenges and opportunities for AFM. *Modern Research and Educational Topics in Microscopy*, 726-733.

Parfondry, A., & Perlin, A. S. (1977). 13C-NMR spectroscopy of cellulose ethers. *Carbohydrate Research*, 57, 39-49. https://doi.org/10.1016/S0008-6215(00)81918-7

Park, S., Baker, J. O., Himmel, M. E., Parilla, P. A., & Johnson, D. K. (2010). Cellulose crystallinity index: measurement techniques and their impact on interpreting cellulase performance. *Biotechnology for Biofuels*, *3*, 1-10. https://doi.org/10.1186/1754-6834-3-10

Peciulyte, A., Kiskis, J., Larsson, P. T., Olsson, L., & Enejder, A. (2016). Visualization of structural changes in cellulosic substrates during enzymatic hydrolysis using multimodal nonlinear microscopy. *Cellulose*, *23*, 1521-1536. https://doi.org/10.1007/s10570-016-0908-z

Pesacreta, T. C., Carlson, L. C., & Triplett, B. A. (1997). Atomic force microscopy of cotton fiber cell wall surfaces in air and water: Quantitative and qualitative aspects. *Planta*, *202*, 435–442. https://doi.org/10.1007/s004250050147

Pettersson, T., Hellwig, J., Gustafsson, P. J., & Stenström, S. (2017). Measurement of the flexibility of wet cellulose fibres using atomic force microscopy. *Cellulose*, *24*, 4139-4149. https://doi.org/10.1007/s10570-017-1407-6

Poletto, M., Ornaghi, H. L., & Zattera, A. J. (2014). Native cellulose: structure, characterization and thermal properties. *Materials*, *7*, 6105-6119. **https://doi.org/10.3390/ma7096105**

Ponz, E., Ladaga, J. L., & Bonetto, R. D. (2006). Measuring surface topography with scanning electron microscopy. I. EZEImage: A program to obtain 3D surface data. *Microscopy and Microanalysis*, *12*, 170-177. https://doi.org/10.1017/S1431927606060028

Prats-Mateu, B., & Gierlinger, N. (2017). Tip in –light on: Advantages, challenges, and applications of combining AFM and Raman microscopy on biological samples. *Microscopy Research and Technique*, *80*, 30-40. **https://doi.org/10.1002/jemt.22744**

Titus, R. N., Staud, C. J., & Gray, H. L. (1932). Microscopy of the cotton cellulose fiber. *Journal of Chemical Education*, *9*, 114. https://doi.org/10.1021/ed009p114

Radhakrishnan, T., Patil, N. B., & Dweltz, N. E. (1969). Crystallite Orientation in Natural Cellulose Fibers. *Textile Research Journal*, *39*, 1003-1014. https://doi.org/10.1177/004051756903901103

Rahman, N. H. A., Chieng, B. W., Ibrahim, N. A., & Rahman, N. A. (2017). Extraction and characterization of cellulose nanocrystals from tea leaf waste fibers. *Polymers*, *9*, 1–11. https://doi.org/10.3390/polym9110588

Rashid, S. and Dutta, H., (2020). Characterization of nanocellulose extracted from short, medium and long grain rice husks. *Industrial Crops and Products*, 154,112627.

Reiterer, A., Jakob, H. F., Stanzl-Tschegg, S. E., & Fratzl, P. (1998). Spiral of elementary cellulose fibrils in cell walls of Picea abies determined by small-angle X-ray scattering. *Wood Science and Technology*, *32*, 335–345.

Revol, J. F., Dietrich, A., & Goring, D. A. I. (1987). Effect of mercerization on the crystallite size and crystallinity index in cellulose from different sources. *Canadian Journal of Chemistry*, *65*, 1724-1725. https://doi.org/10.1139/v87-288

Ricci, D., & Braga, P. C. (2004). Recognizing and avoiding artifacts in AFM imaging. In *Atomic Force Microscopy,* Humana Press, pp. 25-37.

Richards, H. L., Baker, P. G. L., & Iwuoha, E. (2012). Metal Nanoparticle Modified Polysulfone Membranes for Use in Wastewater Treatment: A Critical Review. *Journal of Surface Engineered Materials and Advanced Technology*, *2*, 183–193. https://doi.org/[10.4236/jsemat.2012.223029](http://www.scirp.org/journal/PaperInformation.aspx?PaperID=21428)

Rizal, S., Sadasivuni, K. K., Atiqah, M. N., Olaiya, N. G., Paridah, M. T., Abdullah, C. K., ... & Khalil, H. A. (2021). The role of cellulose nanofibrillated fibers produced with combined supercritical carbon dioxide and high-pressure homogenization process as reinforcement material in biodegradable polymer. *Polymer Composites*, *42*, 1795-1808. **https://doi.org/10.1002/pc.25935**

Rollins, M. L., & Tripp, V. W. (1954). Optical and electron microscopic studies of cotton fiber structure. *Textile Research Journal*, *24*, 345-357. https://doi.org/10.1177/004051755402400407

Rongpipi, S., Ye, D., Gomez, E. D., & Gomez, E. W. (2019). Progress and opportunities in the characterization of cellulose–an important regulator of cell wall growth and mechanics. *Frontiers in Plant Science*, *9*, 1894 - 1906. https://doi.org/10.3389/fpls.2018.01894

Ruangudomsakul, W., Ruksakulpiwat, C., & Ruksakulpiwat, Y. (2015, August). Preparation and characterization of cellulose nanofibers from cassava pulp. *Macromolecular Symposia, 354,* 170 - 176. https://doi.org/10.1002/masy.201400096

Rutland, M. W., Carambassis, A., Willing, G. A., & Neuman, R. D. (1997). Surface force measurements between cellulose surfaces using scanning probe microscopy. *Colloids and Surfaces A: Physicochemical and Engineering Aspects*, *123*, 369-374. https://doi.org/10.1016/S0927-7757(96)03790-9

Sedin, D. L., & Rowlen, K. L. (2001). Influence of tip size on AFM roughness measurements. *Applied surface science*, *182*, 40-48. https://doi.org/10.1016/S0169-4332(01)00432-9

Shak, K. P. Y., Pang, Y. L., & Mah, S. K. (2018). Nanocellulose: Recent advances and its prospects in environmental remediation. *Beilstein Journal of Nanotechnology*, *9*, 2479-2498. https://doi.org/10.3762/bjnano.9.232

Singh, M., Kaushik, A., & Ahuja, D. (2016). Surface functionalization of nanofibrillated cellulose extracted from wheat straw: Effect of process parameters. *Carbohydrate Polymers*, *150*, 48–56. https://doi.org/10.1016/j.carbpol.2016.04.109

Slepkov, A. D., Ridsdale, A., Pegoraro, A. F., Moffatt, D. J., & Stolow, A. (2010). Multimodal CARS microscopy of structured carbohydrate biopolymers. *Biomedical Optics Express*, *1*, 1347-1357. https://doi.org/10.1364/BOE.1.001347

Stevulova, N., Hospodarova, V., & Estokova, A. (2018). Study of thermal analysis of selected cellulose fibres. *GeoScience Engineering*, *62*, 18 - 21. https://doi.org/10.1515/gse-2016-0020

Stiernstedt, J., Brumer, H., Zhou, Q., Teeri, T. T., & Rutland, M. W. (2006). Friction between cellulose surfaces and effect of xyloglucan adsorption. *Biomacromolecules*, *7*, 2147-2153. https://doi.org/10.1021/bm060100i

Stiernstedt, J., Nordgren, N., Wågberg, L., Brumer III, H., Gray, D. G., & Rutland, M. W. (2006). Friction and forces between cellulose model surfaces: A comparison. *Journal of Colloid and Interface Science*, *303*, 117-123. https://doi.org/10.1016/j.jcis.2006.06.070

Szymańska-Chargot, M., Cybulska, J., & Zdunek, A. (2011). Sensing the structural differences in cellulose from apple and bacterial cell wall materials by Raman and FT-IR spectroscopy. *Sensors*, *11*, 5543-5560. https://doi.org/10.3390/s110605543

Szcześniak, L., Rachocki, A. and Tritt-Goc, J., (2008). Glass transition temperature and thermal decomposition of cellulose powder. *Cellulose*, 15, 445-451.

Thygesen, A., Oddershede, J., Lilholt, H., Thomsen, A. B., & Ståhl, K. (2005). On the determination of crystallinity and cellulose content in plant fibres. *Cellulose*, *12*, 563-576. https://doi.org/10.1007/s10570-005-9001-8

Trilokesh, C., & Uppuluri, K. B. (2019). Isolation and characterization of cellulose nanocrystals from jackfruit peel. *Scientific Reports*, *9*, 1-8. https://doi.org/10.1038/s41598-019-53412-x

Trivedi, M. K., Branton, A., Trivedi, D., Nayak, G., Mishra, R., & Jana, S. (2015). Characterization of physicochemical and thermal properties of biofield treated ethyl cellulose and methyl cellulose. *International Journal of Biomedical Materials Research*, 3, 83-91.

Tyler, D. N., & Wooding, N. S. (1958). The determination and the significance of crystallite size in regenerated cellulose fibres. *Journal of the Society of Dyers and Colourists,* 74, 283-291. https://doi.org/10.1111/j.1478-4408.1958.tb02257.x

Vanderghem, C., Jacquet, N., Danthine, S., Blecker, C., & Paquot, M. (2012). Effect of physicochemical characteristics of cellulosic substrates on enzymatic hydrolysis by

means of a multi-stage process for cellobiose production. *Applied Biochemistry and Biotechnology*, *166*, 1423-1432. https://doi.org/10.1007/s12010-011-9535-1

Villares, A., Moreau, C., Bennati-Granier, C., Garajova, S., Foucat, L., Falourd, X., ... & Cathala, B. (2017). Lytic polysaccharide monooxygenases disrupt the cellulose fibers structure. *Scientific Reports*, *7*, 1-9. https://doi.org/10.1038/srep40262

Ward Jr, K. (1950). Crystallinity of cellulose and its significance for the fiber properties. *Textile Research Journal*, *20*, 363-372. https://doi.org/10.1177/004051755002000601

Wickholm, K., Larsson, P. T., & Iversen, T. (1998). Assignment of non-crystalline forms in cellulose I by CP/MAS 13C NMR spectroscopy. *Carbohydrate Research*, *312*, 123-129. https://doi.org/10.1016/S0008-6215(98)00236-5

Wu, H., Chiang, S. W., Lin, W., Yang, C., Li, Z., Liu, J., ... & Wong, C. P. (2014). Towards practical application of paper based printed circuits: capillarity effectively enhances conductivity of the thermoplastic electrically conductive adhesives. *Scientific Reports*, *4*, 1-8. https://doi.org/10.1038/srep06275

Xia, Y., Xu, Y., Li, J., Zhang, C., & Fan, S. (2019). Recent advances in emerging techniques for non-destructive detection of seed viability: A review. *Artificial Intelligence in Agriculture*, *1*, 35–47. https://doi.org/10.1016/j.aiia.2019.05.001

Xiao, C., Zhang, T., Zheng, Y., Cosgrove, D. J., & Anderson, C. T. (2016). Xyloglucan deficiency disrupts microtubule stability and cellulose biosynthesis in Arabidopsis, altering cell growth and morphogenesis. *Plant Physiology*, *170*, 234-249. https://doi.org/10.1104/pp.15.01395

Xu, F., Yu, J., Tesso, T., Dowell, F., & Wang, D. (2013). Qualitative and quantitative analysis of lignocellulosic biomass using infrared techniques: a mini-review. *Applied Energy*, *104*, 801-809. https://doi.org/10.1016/j.apenergy.2012.12.019

Yan, Z., Chen, S., Wang, H., Wang, B., Wang, C., & Jiang, J. (2008). Cellulose synthesized by Acetobacter xylinum in the presence of multi-walled carbon nanotubes. *Carbohydrate Research*, *343*, 73-80. https://doi.org/10.1016/j.carres.2007.10.024

Yarbrough, J. M., Himmel, M. E., & Ding, S. Y. (2009). Plant cell wall characterization using scanning probe microscopy techniques. *Biotechnology for Biofuels*, *2*, 1-11. https://doi.org/10.1186/1754-6834-2-17

Ye, D., Rongpipi, S., Kiemle, S. N., Barnes, W. J., Chaves, A. M., Zhu, C., ... & Gomez, E. D. (2020). Preferred crystallographic orientation of cellulose in plant primary cell walls. *Nature Communications*, *11*, 1-10. https://doi.org/10.1038/s41467-020-18449-x

Zauscher, S., & Klingenberg, D. J. (2000). Normal forces between cellulose surfaces measured with colloidal probe microscopy. *Journal of Colloid and Interface science*, *229*, 497-510. https://doi.org/10.1006/jcis.2000.7008

Zhang, T., Mahgsoudy-Louyeh, S., Tittmann, B., & Cosgrove, D. J. (2014). Visualization of the nanoscale pattern of recently-deposited cellulose microfibrils and matrix materials in never-dried primary walls of the onion epidermis. *Cellulose*, *21*, 853-862. https://doi.org/10.1007/s10570-013-9996-1

Zhang, T., Vavylonis, D., Durachko, D. M., & Cosgrove, D. J. (2017). Nanoscale movements of cellulose microfibrils in primary cell walls. *Nature Plants*, *3*, 1-6. https://doi.org/10.1038/nplants.2017.56

Zhao, H., Kwak, J. H., Zhang, Z. C., Brown, H. M., Arey, B. W., & Holladay, J. E. (2007). Studying cellulose fiber structure by SEM, XRD, NMR and acid hydrolysis. *Carbohydrate Polymers*, *68*, 235-241. https://doi.org/10.1016/j.carbpol.2006.12.013

Zhou, Q., Rutland, M. W., Teeri, T. T., & Brumer, H. (2007). Xyloglucan in cellulose modification. *Cellulose*, *14*, 625-641. https://doi.org/10.1007/s10570-007-9109-0

Zimmerley, M., Younger, R., Valenton, T., Oertel, D. C., Ward, J. L., & Potma, E. O. (2010). Molecular orientation in dry and hydrated cellulose fibers: a coherent anti-Stokes Raman scattering microscopy study. *The Journal of Physical Chemistry B*, *114*, 10200-10208. https://doi.org/10.1021/jp103216j

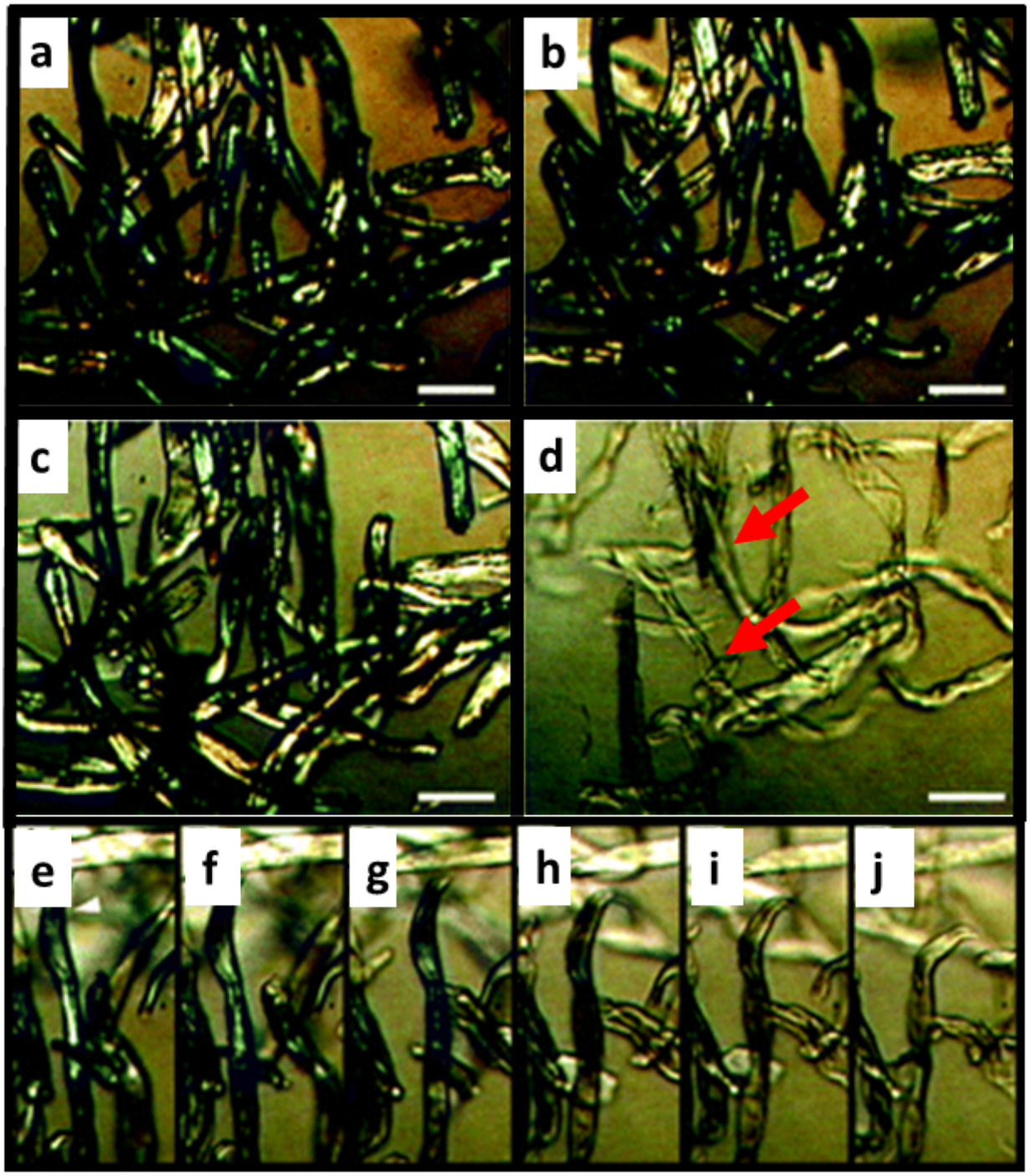

JEMT_24057_fig 2.tif

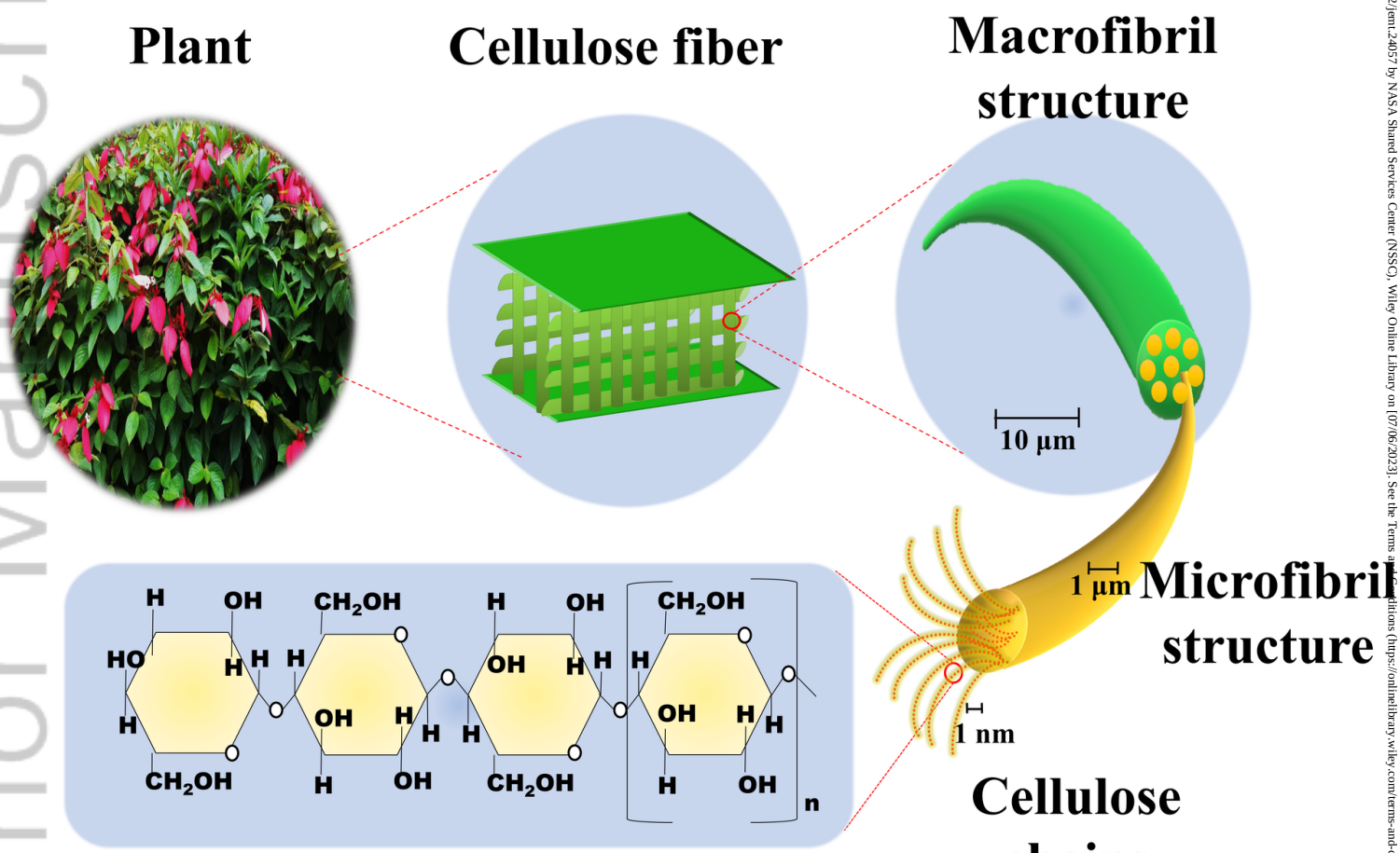

JEMT_24057_Fig 1.tif

JEMT_24057_Fig 3.tif

JEMT_24057_Fig 4.tif

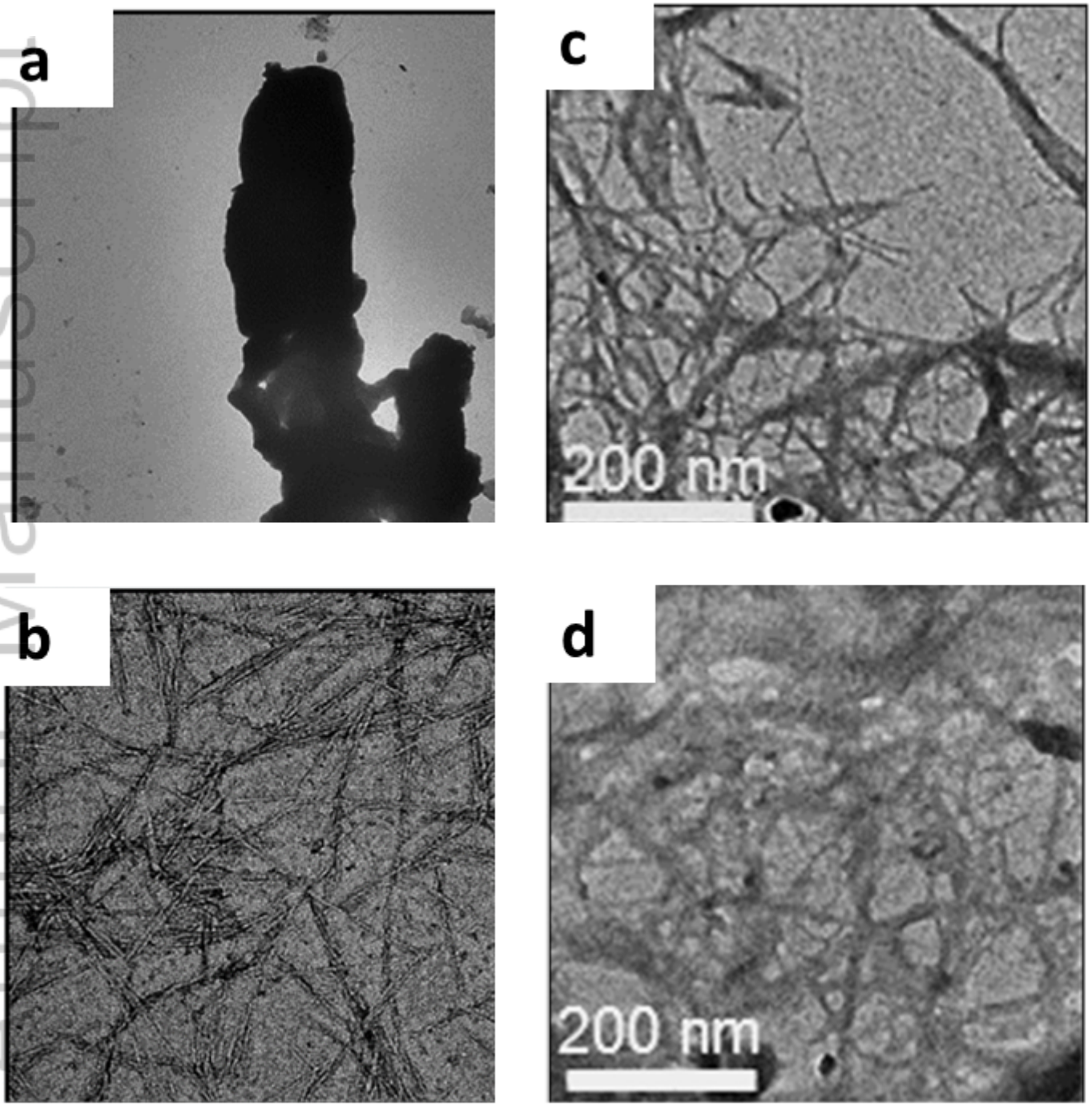

JEMT_24057_Fig 5.tif

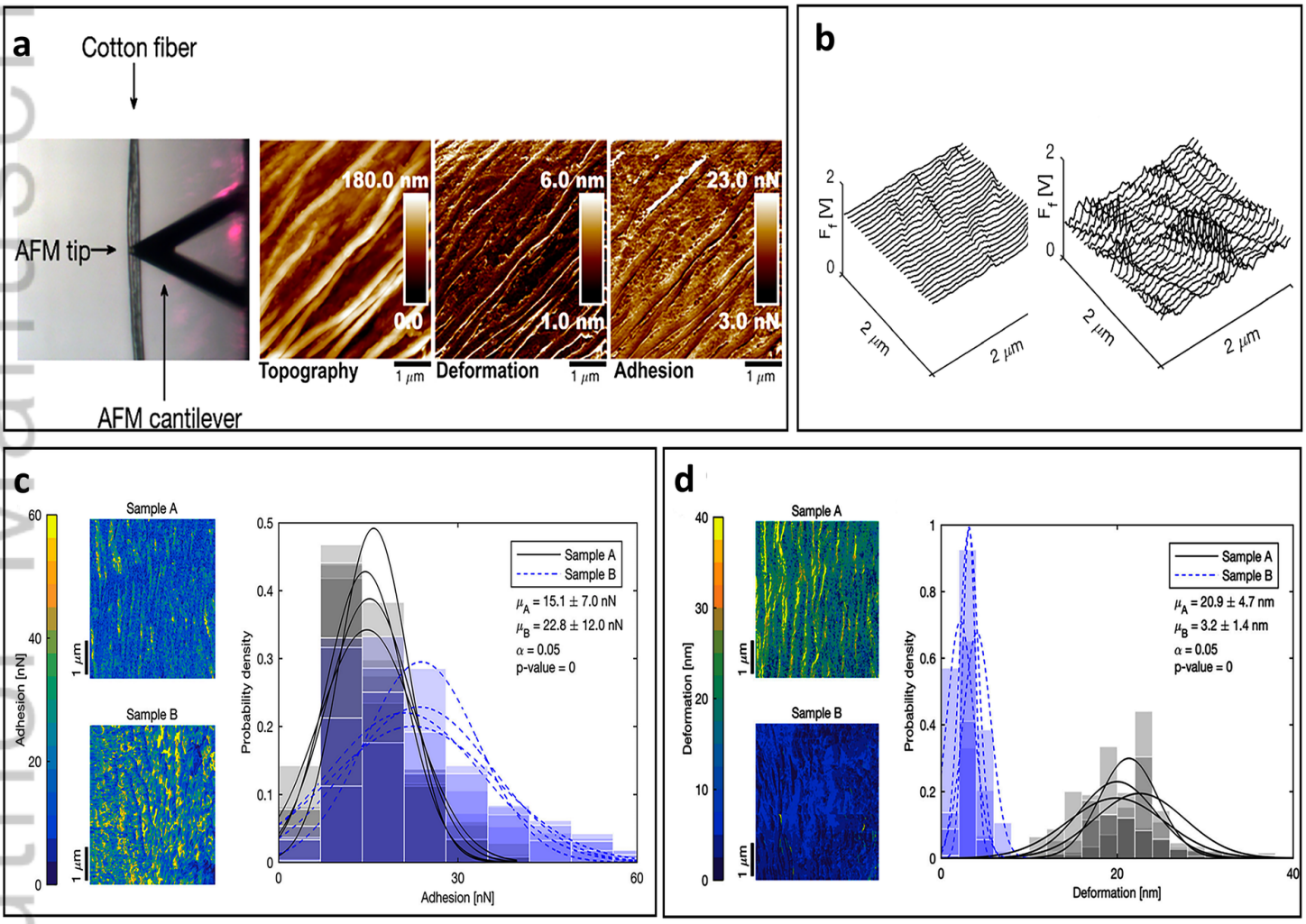

JEMT_24057_Fig 6.tif

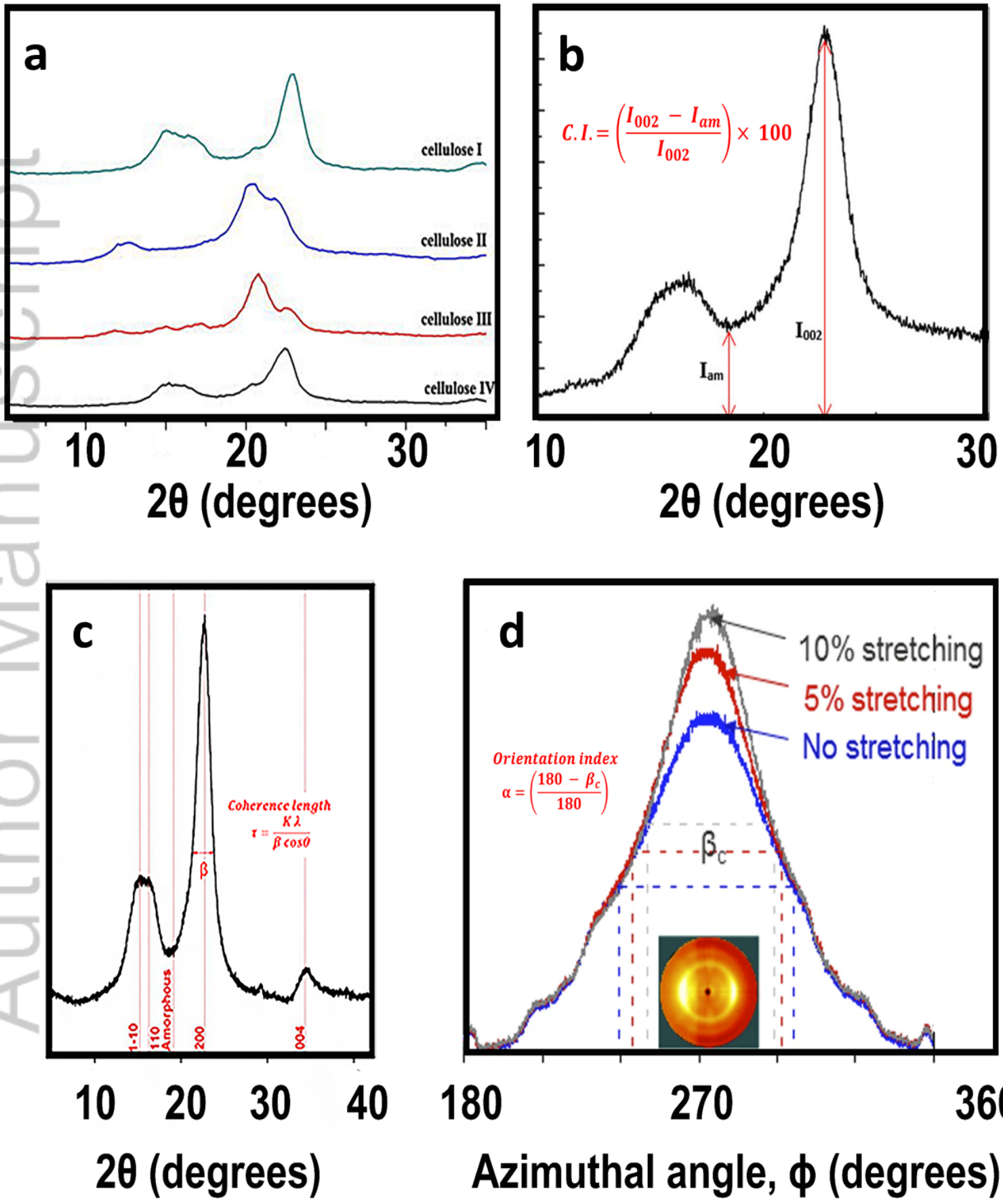

JEMT_24057_Fig 7.tif

JEMT_24057_Fig 8.tif

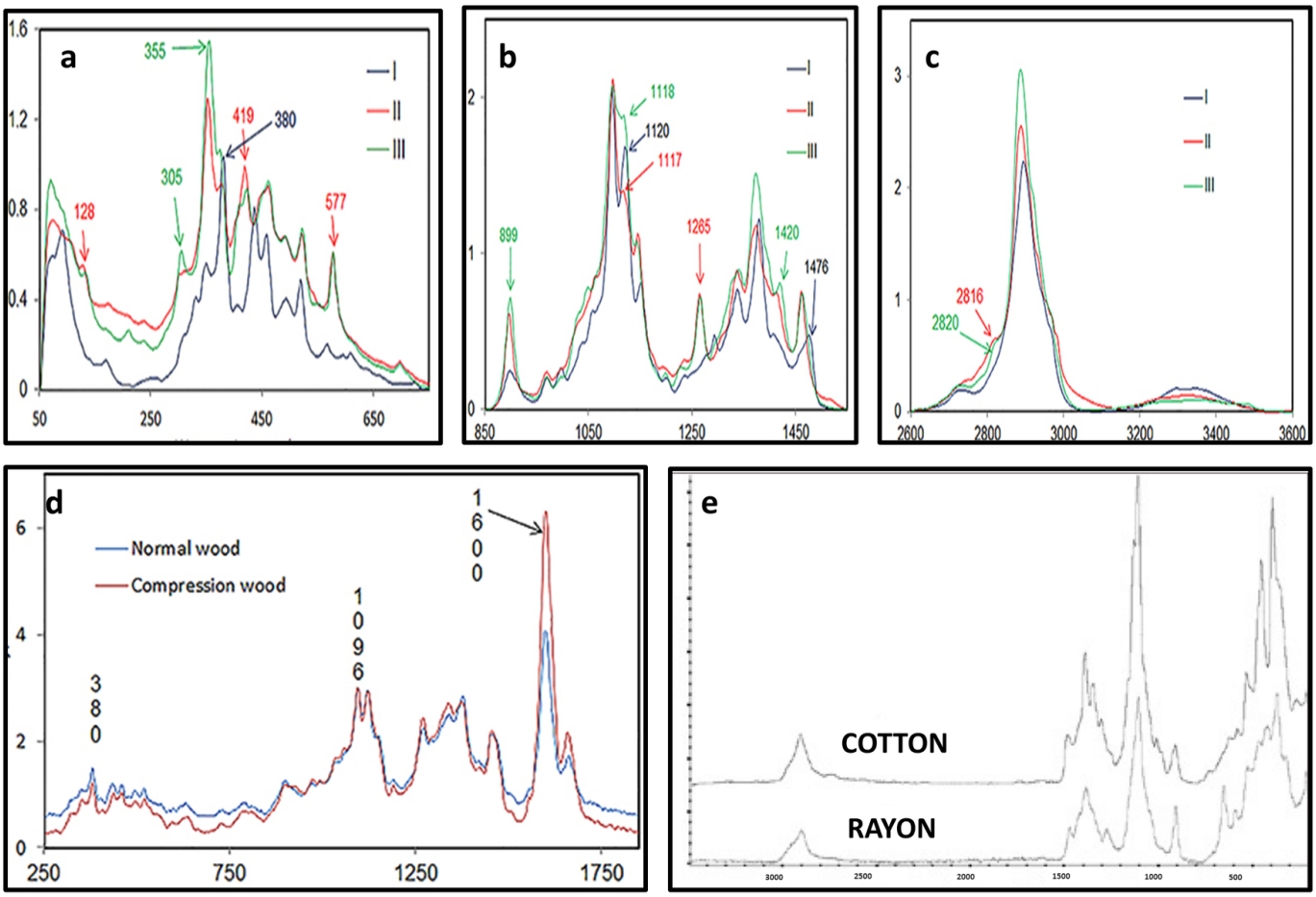

JEMT_24057_Fig 9.tif

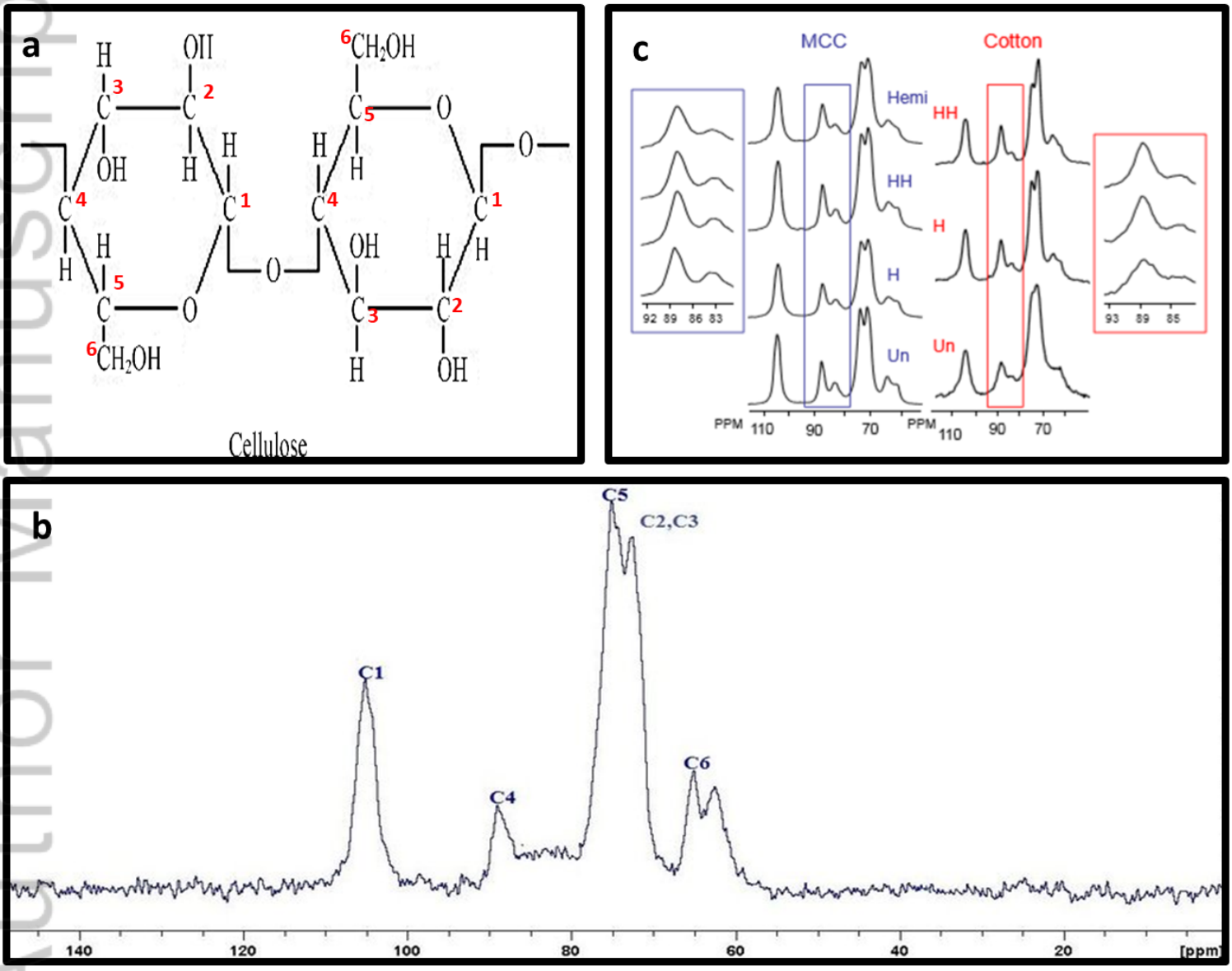

JEMT_24057_Fig 10.tif

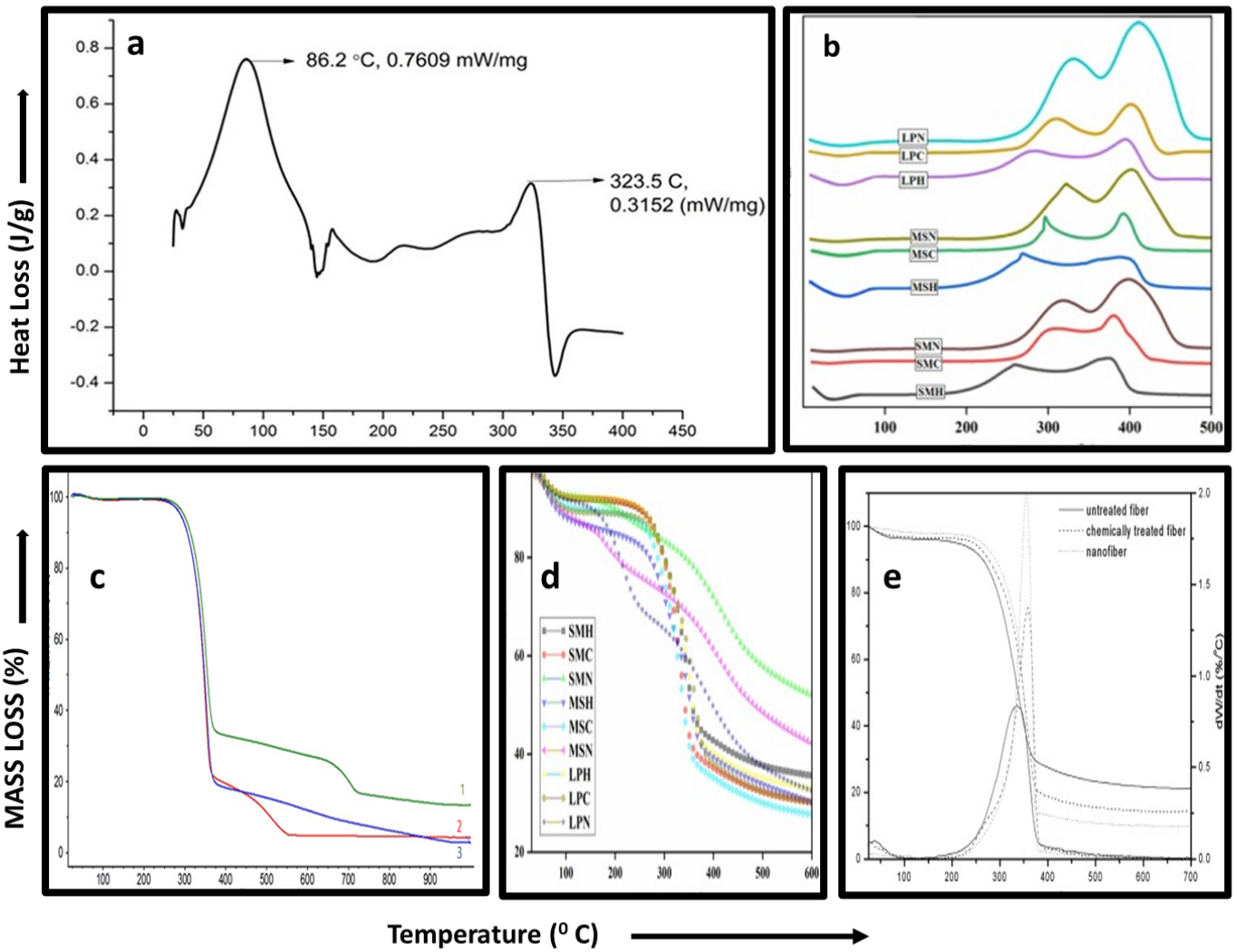

JEMT_24057_Fig 11.tif

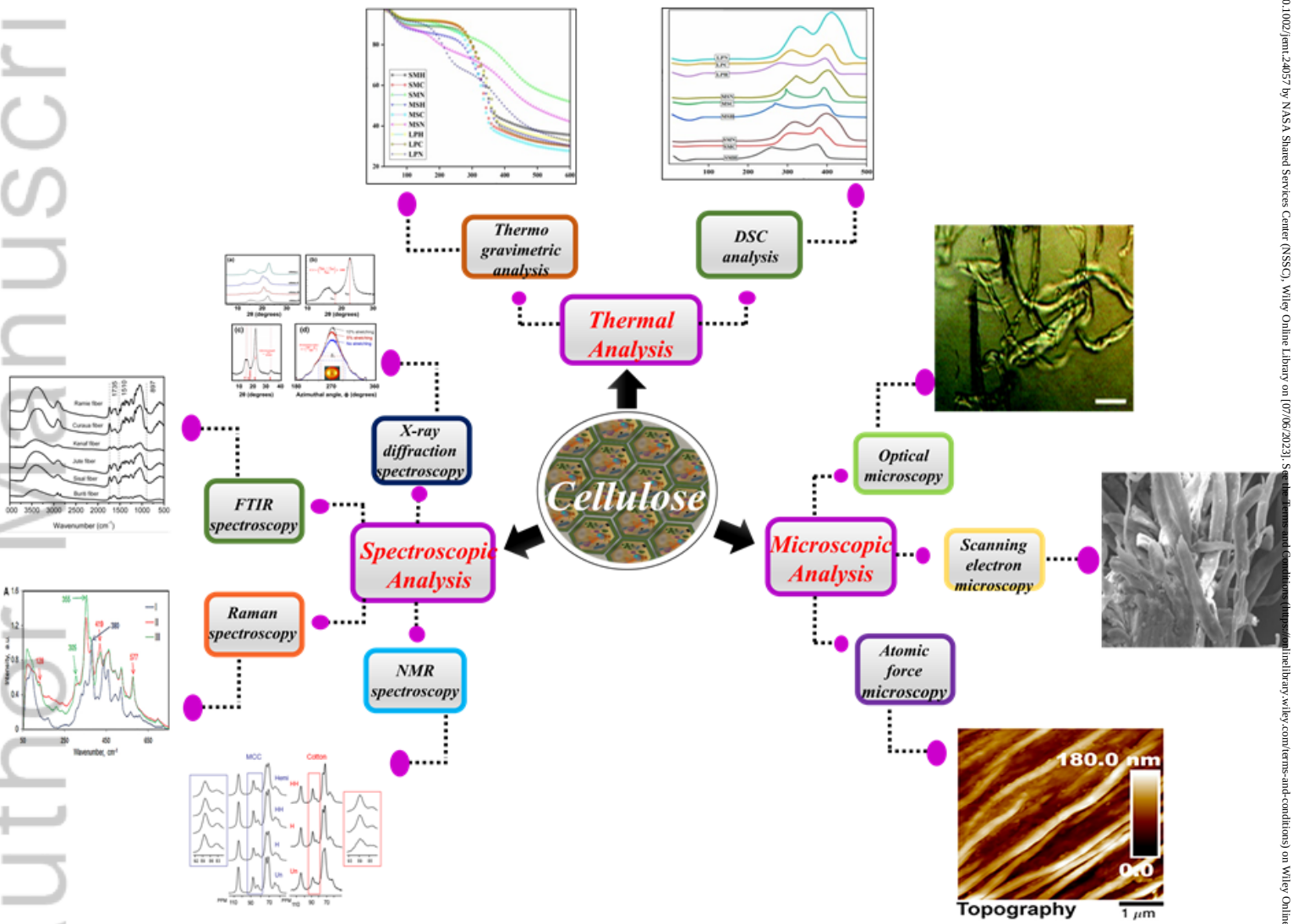

JEMT_24057_graphical abstract.tif

Table 1: Source and characteristics of different cellulose polymorphs (Kroon-Batenburg & Kroon, 1997; Ford et al., 2005; Szcześniak, Rachocki, & Tritt-Goc, 2008)

Type of polymorph	Source	Characteristics studied	Reference
Cellulose I	Naturally occurring	Exists in parallel strands without inter sheet hydrogen bonding	(Kroon-Batenburg & Kroon, 1997)
Cellulose II	Naturally occurs in individual organisms or under specific conditions Mercerization or solubilization of cellulose I	Exists in antiparallel strains with inter sheet hydrogen bonding Thermodynamically more stable	
Cellulose III	Treatment of cellulose I or II with amines	Obtained from decomplexation of ammonia-cellulose I or ammonia-cellulose II	(Ford et al., 2005)
Cellulose IV	Treatment of cellulose III with glycerol at very high temperatures	More symmetrical structure Mixed crystalline habit in which cellulose I and cellulose II conformations co-exist	(Szcześniak, Rachocki, & Tritt-Goc, 2008)

Table 2: Compilation of techniques used to study different characteristics of cellulose from various sources (Chandra et al., 2016; Johar et al., 2012; Ruangudomsakul et al., 2015; Kaushik & Singh, 2011; Cherian et al., 2010; Andrew & Baker et al., 1997; Hosseinali & Thomasson, 2019; Lee et al., 2000; Ju, Bowden, Brown, & Zhang, 2015; Doh, Lee, Lim, & Im, 2013; Hospodarova et al., 2018; Kavkler & Demšar, 2012; Foston et al., 2011; Vivian Abiaziem et al., 2019; Trilokesh & Uppuluri, 2019; Trivedi et al., 2015; Kolářová et al., 2013; Deepa et al., 2011; Issa, Abou-Sekkina, Khedr, Bastawisy, & El-Helece, 2016; Awal et al., 2010; Szcześniak et al., 2008; Dahiya & Rana, 2004)

Electron Microscopy: Morphology

Cellulose source	Characteristics studied	Reference
Arecanut husk	• Uneven surface • Presence of binding materials like hemicelluloses, lignin, pectin	(Chandra et al., 2016)
Rice husk	• Smooth surface • Hemicelluloses, lignin, pectin, wax, and other impurities	(Johar et al., 2012)
Cassava pulp	• Smooth and clear surface post bleaching • Absence of lignin	(Ruangudomsakul et al., 2015)
Wheat straw	• Removal of hemicelluloses, lignin, and pectin after steam explosion • Reduction in particle size	(Kaushik & Singh, 2011)
Pineapple leaf fibre	• Fibrils are associated in bundles • Smooth surface	(Cherian et al., 2010)

AFM: Surface topography

Cellulose source	Mode	Characteristics studied	Reference
Valonia cellulose I microcrystals	Contact	• Surface topography (height and deflection of image)	(Andrew Baker et al., 1997)
Cotton fibres	Contact	• Surface topography	

		• Friction images	(Hosseinali & Thomasson, 2019)
	Force tapping	• Nanomechanical properties (adhesion and deformation)	
Cotton fibre incubated with CBH I (cellulase)	Tapping	• Effect of cellulase components action on the surface of cotton fibres	(Lee et al., 2000)
Cotton fibre incubated with EG II (cellulase)	Tapping		

XRD: Ultrastructure and Crystallinity

Cellulose source	**Characteristics Studied**	**Reference**
Nanocrystalline cellulose (NCC) from bleached wood pulp	Crystallinity Index: 90%, Segal method	(Ju, Bowden, Brown, & Zhang, 2015)
Avicel	Crystallinity Index: 88%, Segal method	
Carboxymethyl cellulose (CMC)	Decrease in crystallinity was shown as three typical crystalline peaks of Cellulose I structure at diffraction angles (14.5°, 22.4°, and 34.0°) disappeared after carboxymethylation	(Doh, Lee, Lim, & Im, 2013)

Vibrational Spectroscopy

Cellulose source	**Technique**	**Bands for cellulose in Vibrational spectroscopy**	**Reference**
Wood pulp and recycled wastepaper	FTIR	O-H,C-H, CH_2 , -CH, -OH and C-O bonds	(Hospodarova et al., 2018)
Cotton	Raman	CH_2, CO, CCC ring,	(Kavkler & Demšar, 2012)
	FTIR	CH, CH_2, CHO, COH, OH, CH, COC	

NMR:chemical composition

Cellulose source	Characteristics studied	Reference
Cellulose from biomass	• Effects of holocellulose pulping and hemicellulose removal by acid hydrolysis on the crystalline ultrastructural components of cellulose	(Foston et al., 2011)
Cellulose nanocrystal of sugarcane peel	• Six carbon atoms of cellulose and the disappearance of several signals indicating disruption of the amorphous region • Majority of the carbohydrates were taken off during treatment with the acid	(Vivian Abiaziem et al., 2019)

DSC: Gelatinization

Cellulose source	Tp (°C)	ΔH	Type of peak	Reference
Jackfruit peel	323.5	0.3152 mW/mg	Endothermic	(Trilokesh & Uppuluri, 2019)
Cellulose powder	74	72 (J/g)	Endothermic	(Trivedi et al., 2015)
Ethyl cellulose	334.46	1.10 kJ/g	Exothermic	(Kolářová et al., 2013)
Cotton cellulose	315	7.65(J/g)	Exothermic	(Dahiya & Rana, 2004)
Raw banana fibre	350	35.7(J/g)	Exothermic	(Deepa et al., 2011)
Acid treated banana fibre	113.7	1279(J/g)	Endothermic	

TGA: Thermal stability

Cellulose source	Temperature range (°C)	Weight loss (%)	Reference
Rice straw pulp	35-100	11.80	(Issa, Abou-Sekkina, Khedr, Bastawisy, & El-Helece, 2016)
	300-325	30.35	
	470-1000	25.62	

Wood pulp	35- 230	5.966	(Awal et al., 2010)
	230-390	76.36	
	370-483	-	
Jackfruit peel	35-150	7	(Trilokesh & Uppuluri, 2019)
	200-380	85	
	Above 380	-	
Cellulose powder	36-120	7	(Szcześniak et al., 2008)
	220-300	62	
	300-475	28	
Ethyl cellulose	280-380	80.45	(Trivedi et al., 2015)
Cotton cellulose	170-300	11.11	(Dahiya & Rana, 2004)
	300-355	71.20	
	355-580	24.1	